Isolation and Gene Flow in a Speciation Continuum in Newts

M. Pabijan*[1,2], P. Zieliński[1], K. Dudek[1], M. Stuglik[1,3], W. Babik*[1]

[1]*Institute of Environmental Sciences, Jagiellonian University, ul. Gronostajowa 7, 30-387, Kraków, Poland*

[2]*Department of Comparative Anatomy, Institute of Zoology, Jagiellonian University, ul. Gronostajowa 9, 30-387, Kraków, Poland*

[3]*Scotland's Rural College, Integrative Animal Sciences, Easter Bush Campus, Midlothian EH25 9RG, Scotland, UK*

Key Words: delimitation, reticulate evolution, taxonomy, amphibian

* corresponding authors

Corresponding authors:

Maciej Pabijan, Department of Comparative Anatomy, Institute of Zoology, Jagiellonian University, ul. Gronostajowa 9, 30-387, maciej.pabijan@uj.edu.pl

Wiesław Babik, Institute of Environmental Sciences, Jagiellonian University, ul. Gronostajowa 7, 30-387, Kraków, Poland**;** wieslaw.babik@uj.edu.pl

Running title: Species delimitation and gene flow in newts

Abstract

The evolution of reproductive isolation is a prolonged process that fosters genetic exchange between differentiating metapopulation lineages. Gene flow between incipient species provides an opportunity to quantify and understand the impact of gene flow on the accumulation of divergence along the speciation continuum. Here we delimit taxa, reconstruct phylogeny and infer gene flow in newts of the *Lissotriton vulgaris* species complex based on 74 nuclear markers sequenced for 127 populations. Using several species delimitation and phylogenetic methods, we recovered nine allo- and parapatric taxa, and obtained a partially resolved phylogeny. Approximate Bayesian Computation modeling detected historical and recent gene flow between several taxa, including non-sister pairs. Gene flow among taxa in Central Europe (*L. v. ampelensis*, *L. v. meridionalis*, two morphologically cryptic taxa within *L. v. vulgaris*) suggests that these lineages are non-independent and possibly in the process of merging in some areas. Three southern lineages (*L. v. graecus*, *L. v. kosswigi*, *L. v. lantzi*) have acquired the population genetic hallmarks of independent species, whereas the status of *L. v. schmidtleri* remains uncertain. We identified hybridization, causing extensive haplotype sharing between non-sister lineages, as an important source of genealogical discordance, positively misleading multispecies coalescent-based species tree methods. We also obtained strong statistical support for widespread mtDNA introgression, suggested by previously observed discordance between mtDNA phylogeny and morphology. Our study shows that distinct metapopulation lineages along the speciation continuum can exchange nontrivial amounts of genes and emphasizes an urgent need for effective methods accounting for gene flow in species tree reconstruction.

Introduction

Speciation, regardless of the mechanisms or geographic settings in which it occurs, is typically a gradual process (Coyne & Orr 2004). The consequences of this are manifold. First, we see various stages of speciation in nature which makes delimitation of separately evolving units challenging (Wiens 2007; Huang & Knowles 2016). Second, completion of speciation is by no means certain, other outcomes such as fusions or extinction are also likely (e.g. Rhymer & Simberloff 1996; Rudman & Schluter 2016). Gene flow may homogenize diverging gene pools (Slatkin 1985; Petit & Excoffier 2009), thereby limiting or even reversing differentiation. Third, it remains to be seen to what extent diagnosable metapopulation lineages evolve separately with respect to sharing adaptively significant genetic variation (Rieseberg & Burke 2001; Rieseberg *et al.* 2004). Fourth, it is unclear how much "neutral" gene flow occurs between differentiating lineages, whether contact between such lineages causes massive introgression, and to what extent introgression is heterogeneous throughout the genome (Cruikshank & Hahn 2014; Wolf & Ellegren 2016).

Although theory provides some guidelines, the preceding questions are mostly empirical and need to be addressed by studying natural systems. Recent spectacular adaptive radiations may be less informative and more exceptional in this respect than commonly assumed, because extinction may not have yet had sufficient time to prune the more ephemeral products of divergent selection (Cutter & Gray 2016). Therefore, careful analyses of taxa composed of metapopulation lineages at various stages of divergence (de Queiroz 2007), which can be referred to as a speciation continuum, are needed. Because the necessary analyses lie at the interface of population genetics and phylogenetics, they require integration of tools from both fields. This is especially important for studies that explicitly incorporate gene flow into the equation, because population genetic approaches for inferring post-divergence gene flow are better developed than methods co-estimating phylogeny and gene

flow (Sousa & Hey 2013). Likewise, accounting for post-divergence gene flow is a major challenge for current species delimitation methods (Petit & Excoffier 2009).

European newts from the *Lissotriton vulgaris* group may provide an empirical example of a speciation continuum influenced by genetic exchange between taxa. The Carpathian newt, *L. montandoni* (Boulenger, 1880) and the smooth newt, *Lissotriton vulgaris* (Linnaeus, 1758), have parapatric distributions in central Europe (Fig. 1a; Rafiński & Arntzen 1987; Macgregor *et al.* 1990). The former is endemic to the Carpathian mountains, whereas the latter has a very large range in Central and Northern Europe, with a disjunct population surrounding the Greater Caucasus mountains (Fig. 1a). At the intraspecific level, *L. montandoni* is morphologically uniform across its range, mirrored by only shallow genetic substructuring (Zieliński *et al.* 2014). In sharp contrast, *L. vulgaris* is morphologically differentiated into at least seven subspecies (Fig. 1a; Raxworthy 1990). The smooth newt is found in a variety of habitats across the collective ranges of the subspecies (Bousbouras & Ioannidis 1997; Bour *et al.* 2002; Schmidtler & Franzen 2004; Skorinov *et al.* 2008) from deciduous woodlands, farmlands and pastures in European lowlands and mountainous regions, forest-steppe and taiga in western Siberia and Kazakhstan and pockets of humid habitat in otherwise dry woodland or scrub in southern Europe and Anatolia. Despite over a century of study, the status of the *L. vulgaris* subspecies is still controversial (Schmidtler & Franzen 2004; Dubois & Raffaëlli 2009; Speybroeck *et al.* 2010; Wielstra *et al.* 2015). The disagreement has been exacerbated by a general lack of concordance between morphologically assessed subspecific boundaries and spatial patterns of mtDNA variation (Fig. 1a, Fig. S1; Babik *et al.* 2005; Nadachowska & Babik 2009; Pabijan *et al.* 2015). The traits used to distinguish the smooth newt subspecies pertain almost exclusively to male secondary sexual characters, which include the presence/absence and extent of dorsal crests and tail fins, toe flaps, tail filament, dorso-lateral ridges and pigmentation patterns

(Raxworthy 1990) that develop in aquatic habitat during the breeding season. Despite divergent courtship behavior (Pecio & Rafiński 1985) that leads to strong but incomplete prezygotic sexual isolation between *L. montandoni* and *L. vulgaris* (Michalak *et al.* 1997; Michalak & Rafiński 1999), these two species hybridize in and around the Carpathian mountains forming a bimodal hybrid zone (Kotlík & Zavadil 1999; Babik *et al*. 2003; Babik & Rafiński 2004). Hybridization has led to the replacement of the original mtDNA of *L. montandoni* by introgressed mtDNA of several *L. vulgaris* lineages (Babik *et al*. 2005; Zieliński *et al*. 2013). Moreover, genetic exchange among the different subspecies of *L. vulgaris* is suggested because five of the subspecific taxa do not form monophyletic mtDNA lineages (Fig. S1; Babik *et al*. 2005; Nadachowska & Babik 2009; Pabijan *et al*. 2015). Areas of subspecies intergradation with morphological intermediates have been reported in central and southeastern Europe (e.g. Schmidtler & Schmidtler 1983; Krizmanic *et al*. 1997; Schmidtler & Franzen 2004; Wielstra *et al*. 2015). These findings suggest that introgressive hybridization both between *L. vulgaris* and *L. montandoni*, and among the various subspecies of *L. vulgaris*, has the potential to blur boundaries among the different taxa.

Here, we provide a multi-faceted perspective on the stages of divergence in the *L. vulgaris* complex. First, we postulate that morphologically diagnosable taxa within the complex constitute separately evolving metapopulation lineages (de Quieroz 2007) and test this assertion using a clustering approach based on allele frequencies, a Bayesian multispecies coalescent delimitation method, and the genealogical sorting index. Second, we hypothesize that extensive reticulation has occurred in the evolutionary history of the *L. vulgaris* complex, with the potential to mislead multispecies coalescent-based species tree reconstruction (Leaché *et al.* 2014; Solís-Lemus *et al*. 2016). This issue is addressed by including phylogenetic methods based on concatenation, concordance and a method that explicitly takes reticulation into account. Third, we predict that the extent of historical gene flow was most

extensive among lineages inhabiting Central Europe, and use an Approximate Bayesian Computation framework to model gene flow between pairs of taxa. Finally, we apply the inferred nuclear phylogeny to statistically test the previously proposed hypothesis of extensive mtDNA introgression among morphologically diagnosable taxa. We demonstrate that isolation in space and time as well as post-divergence gene flow shape the genetic background of a set of metapopulations that have diverged in ecology and morphology including male epigamic traits.

Materials and Methods

Newt Sampling

Tissues (tail-tips) were sampled from 127 newt populations (i.e. breeding sites, Table S1 and Fig. 1b). Our sampling focused on capturing the genetic variation present in all morphologically defined taxa within the *L. vulgaris* group and all potential Pleistocene refugia (Babik *et al.* 2005; Nadachowska & Babik 2009; Pabijan *et al.* 2015) and was therefore mostly limited to southeastern and central Europe. One individual was sampled per locality. Altogether we analysed sequence data for 128 individuals (plus outgroup) which included 42 reported in Zieliński *et al.* (2016) and 87 sequenced for this study (Table S1).

Laboratory Procedures and Datasets

DNA from ethanol preserved tissues was extracted using either a standard phenol/chloroform technique or the Wizard Genomic DNA extraction kit (Promega). Amplification and sequencing of a panel of 74 nuclear, mostly 3'UTR markers, followed Zieliński *et al*. (2014). This procedure resulted in physically phased sequences of both haplotypes for most markers in most individuals. We used five different datasets for analyses (Table S2) i) dataset 1 with all 74 loci and all 128 individuals, ii) dataset 2 with all 74 loci but with 118 individuals

(excluded 9 admixed individuals and one of two newts from locality Kapakli), iii) dataset 3 with all 128 individuals but 70 loci (excluded 4 loci with > 10% missing sequences), iv) dataset 4 consisting of SNPs from 71 loci (excluded loci with >10% missing data at nucleotide positions) and 120 individuals (including outgroup).

Species Delimitation

Species delimitation was based on identifying distinct genetic groups from haplotype frequency data and validating the putative OTUs (operational taxonomic units) using multispecies coalescent-based and genealogical sorting methods.

Sequence alignments (dataset 1) were converted into input for STRUCTURE v.2.3.4 (Pritchard *et al.* 2000) by coding each haplotype as a unique integer in a custom Python script. If nucleotide sequences contained over 10 Ns or gaps, they were coded as missing data, if they had less than 10 Ns or gaps, then columns with missing data were removed from the alignment. This procedure ensured that haplotype identity was based on nucleotide differences between sequences (and not on e.g. indels or low-quality data) and provided a conservative estimate of the number of haplotypes per locus. STRUCTURE was run under the admixture model ($\alpha = 1.0$) with independent allele frequencies among populations ($\lambda = 1.0$) for K from 1 to 12, iterated 10 times each. The Markov chain in each analysis was set to 1 million burnin steps; a further 2 million steps were used for parameter value estimation. STRUCTURE HARVESTER (Earl & vonHoldt 2012) and CLUMPAK (Kopelman *et al.* 2015) were used process the STRUCTURE output and to evaluate the most probable number of clusters (K) by examining logPr(*Data*).

We validated the genetic clusters identified by STRUCTURE by applying joint Bayesian species delimitation and species tree estimation using the program BPP v3.1 (Yang 2015). This approach is based on the multispecies coalescent and compares different models

of species delimitation and species phylogeny in a Bayesian framework, accounting for incomplete lineage sorting and gene tree-species tree conflict (Yang & Rannala 2010; Rannala & Yang 2013; Yang & Rannala 2014). Input alignments were constructed from dataset 2 by taking 10 sequences per marker for each of the 9 STRUCTURE-defined genetic clusters (i.e., operational taxonomic units, OTUs). This sampling strategy was based on the minimum number of sequences available per taxon (imposed by 5 specimens of *L. v. meridionalis*), with random subsampling of 10 sequences (without replacement) in all other taxa. Admixed individuals (as defined by STRUCTURE) were excluded from this analysis. We explored a wide variety of priors on the population size parameters (θs) and divergence time at the root of the species tree (τ_0) (see Extended Methods in the Supplementary Material).

Next, we estimated gene trees in MrBayes 3.2 (Ronquist *et al.* 2012), and used them as input to assess genealogical sorting and in Bayesian concordance analysis (see below). We applied dataset 3; outgroups consisted of a single, randomly chosen haplotype per locus of a *Lissotriton helveticus* individual, or if unavailable due to lack of amplification, a single haplotype from either *L. italicus* (for 3 markers) or *L. boscai* (for 9 markers) from Zieliński *et al.* (2014). Nucleotide substitution models for each marker were determined in jModeltest 2.1.4 (Darriba *et al.* 2012) under the Bayesian information criterion. Due to the low phylogenetic information content for many of the analyzed loci, we did not partition the alignments into codon positions for those markers in coding regions. We implemented two runs each with four chains for 3 million generations with trees and parameters sampled every 3000 generations. Convergence was assessed by comparing the –lnL values between runs and by examining parameter values for a subset of markers in Tracer (Rambaut & Drummond 2007). We discarded half of recorded gene trees as burnin, combined runs and constructed an extended majority tree in MrBayes (allcompat command).

We quantified the genealogical distinctiveness of the STRUCTURE-delimited OTUs by measuring exclusive ancestry across gene trees with the genealogical sorting index (*gsi*) of Cummings *et al.* (2008). This statistic measures the genealogical exclusivity of a grouping on a scale from 0 (random distribution of sequences among groups) to 1 (complete monophyly), and an ensemble statistic (*egsi*) is used to integrate across gene trees. Because the *gsi* is sensitive to disparity in group size, we randomly pruned leaves to a sample size of 10 for each OTU. Admixed individuals were also pruned from gene trees. We used the R implementation of the *gsi* (genealogicalSorting v.0.92). The null hypothesis that the degree of exclusive ancestry of each group was observed by chance was evaluated by 10^6 permutations.

Phylogeny Estimation

Our first phylogenetic approach involved using individuals as OTU's (operational taxonomic units) and concatenating the sequences of all loci. This procedure necessitates the selection of a single haplotype per individual per marker and becomes non-trivial if an OTU is heterozygous at multiple loci, because the choice of which haplotype to concatenate into the matrix may influence both the topology and branch support of resultant trees (Weisrock *et al.* 2012). For each individual in dataset 2, we randomly merged haplotypes from each gene into two concatenated sequences (i.e., each individual was represented by two entries of 36, 918 bp consisting of 74 concatenated markers). We then pooled haplotypes for each candidate species and randomly selected half of the haplotypes from each group for analysis. We followed Weisrock *et al.* (2012) in conducting ten replicate analyses to assess consistency. We ran mixed-model phylogenetic analyses in MrBayes 3.2 on the CIPRES Science Gateway platform (Miller *et al.* 2010). We divided the alignments into 74 partitions corresponding to markers and assigned the optimal nucleotide substitution models to these partitions as previously determined by jModeltest. Each analysis consisted of two runs with 8 chains for 20 million generations with trees and parameters sampled every 5000 generations; burnin was set

194 at 50%. Convergence between runs was assessed by examining effective samples sizes and
195 parameter values between rubs in Tracer, and by comparing topologies in AWTY (Nylander
196 *et al.* 2008).

197 The second phylogenetic method involved using BUCKy (Ané *et al.* 2007; Larget *et*
198 *al.* 2010) to estimate levels of concordance in reconstructed topologies among the posterior
199 distributions of gene trees generated in MrBayes. Because the number of unique tips per gene
200 tree was prohibitive (see Extended Methods), we pruned the gene trees in the MrBayes
201 posterior distributions by randomly selecting a single tip from each OTU using an R script
202 from Weisrock *et al.* (2012), modified to accommodate our dataset and subsampling
203 requirements. Admixed individuals were also pruned from gene trees. We tested a range of
204 priors and parameter values for BUCKy (see Extended Methods). We pruned the original
205 gene trees to 10 OTUs (9 candidate species plus outgroup) and repeated the subsampling and
206 pruning routine 50 times, using BUCKy to calculate the primary concordance trees for each
207 replicate. We measured clade support by calculating the mean (± SD) sample-wide
208 concordance factors for clades across all 50 replicates. We also measured clade support by
209 computing the frequency with which each clade was recovered over all replicates.

210 The *BEAST module of BEAST v2.1.3 (Heled & Drummond 2010; Bouckaert *et al.*
211 2014) was used to infer a species tree using the STRUCTURE-defined candidate species. To
212 increase the efficiency of the MCMCs and decrease run times, we minimized the complexity
213 of the estimated parameters (see Extended Methods) and randomly subsampled two gene
214 copies from each *Lissotriton* lineage across the 74 alignments (dataset 2). Because these runs
215 used only 18 (7.6% of total number) of the gene copies available per marker per analysis, we
216 repeated the random selection procedure 10 times, constructing 10 input files. Each analysis
217 was run twice for 10^9 generations. After removing 20% burnin from species tree posteriors,
218 we scaled down the files by taking every eighth tree from the posterior, leaving 2000 trees

from each run. The posterior species trees were combined for replicate runs in LogCombiner v2.1.3, summarized as maximum clade credibility trees in TreeAnnotator v2.1.2, and visualized in DensiTree v2.1.11 (Bouckaert 2010).

Genetic divergence and haplotype sharing

We concatenated all sequences in dataset 2 (without admixed individuals) and used DnaSP v5 (Librado & Rozas 2009) to calculate d_{xy} values among the newt OTUs. The pattern of shared variation was summarized by counting the numbers of shared haplotypes between among OTUs in a custom Python script also using dataset 2.

TreeMix analyses

We constructed a maximum likelihood tree using TreeMix 1.12 (Pickrell & Pritchard 2012) which uses a covariance matrix based on allele frequencies of SNPs to infer the evolutionary relationships among pre-specified populations. The algorithm then identifies populations more closely related than predicted by the phylogeny and adds a “migration edge” between them, representing the direction and magnitude of gene flow (Pickrell & Pritchard 2012). We used the nine Structure-delimited OTUs and an outgroup as populations. Note that allele frequencies for our outgroup “population” were based on two gene copies because only one outgroup individual was sequenced per marker (see single gene analyses above). We extracted and sorted biallelic SNPs at each of the 74 markers according to minor allele frequency (MAF). Five SNPs with the highest MAF, i.e. most informative at the level of the entire dataset, were retrieved per marker, under the condition that they contained <10% missing data at a nucleotide position; these positions were then converted to TreeMix format using a custom Python script. A total of 71 out of 74 markers met our criteria, resulting in a matrix of 355 SNPs (dataset 4). TreeMix was invoked with –k 5 to account for linkage disequilibrium for SNPs from the same marker. In consecutive analyses, we added from one to five

migration edges to allow for gene flow in the tree. We also ran TreeMix with an alternative dataset using only 1 SNP per marker with the highest MAF.

Gene flow among OTUs modeled by ABC

We estimated gene flow between all pairs of taxa (36 pairwise comparisons) in an Approximate Bayesian Computation (ABC) framework. We followed Zieliński *et al.* (2016) in removing all fully coding markers from analyses and also excluded all missing data by removing loci or individuals in pairwise comparisons; final datasets included 60-66 loci with between 5 and 24 sequences per taxon (Table S3). The information present in the data was summarized for each pairwise comparison with a set of 9 summary statistics (Table S3 and Extended Methods).

We tested four simple scenarios of pairwise species divergence and the extent and timing of interspecific gene flow: i) a no gene flow (NGF) model in which an ancestral population splits into two at time T_{SPLIT} with no genetic exchange between descendant populations, ii) an admixture (ADM) model in which a fraction of genes is moved instantaneously from one population to the other; this can occur once independently in each direction at any time after divergence, iii) a constant gene flow (CGF) model in which gene flow is continuous and bidirectional between descendent taxa after T_{SPLIT}, and iv) a recent gene flow (RGF) model in which continuous and bidirectional gene flow between descendent taxa was constrained to have occurred in the last 200,000 years (approximately 50,000 newt generations).

Coalescent simulations were done in fastsimcoal2.01 (Excoffier *et al*. 2013), and the ABC analysis was conducted within the ABCtoolbox (Wegmann *et al*. 2010). Detailed prior and parameter values are given in the Extended Methods. A total of 10^6 datasets were simulated under each demographic model from which we retained 1% (10^4) best simulations

and computed the marginal likelihood of the observed and retained datasets under the generalized linear model (Leuenberger & Wegmann 2010). To control the type I error for multiple comparisons, we used a Bonferroni correction and removed models with the nominal $P<0.0125$. The best fitting model was then selected via Bayes factors.

We estimated the power to distinguish between the four models within the ABC framework by randomly picking 1000 pseudo-observed datasets from all simulations generated for each model and checking how often the ABC procedure correctly predicted the true model (the one that produced the dataset). Each pseudo-observed dataset was treated as the observed data and used to calculate marginal densities of all compared models; Bayes factors were used to select the best model. Because identical prior distributions were used for all pairwise comparisons, we conducted a single power analysis using populations with the fewest sequences (*L. v. meridionalis* - *L. v. kosswigi*). This can be considered the minimum estimate as all other comparisons (with larger sample sizes) will have more power in distinguishing between models.

Statistical test of mtDNA introgression

We formally tested whether the sharing of mtDNA haplotypes among *Lissotriton* groups could be accounted for by ILS (incomplete lineage sorting) or is due to hybridization. We assumed that the (partially) resolved nuclear phylogeny reflects true relationships among the evolutionary lineages within *L. montandoni*/*L. vulgaris* and followed the statistical approach of Joyce *et al*. (2011). If mtDNA similarities among evolutionary lineages result from ILS, then mtDNA sequences simulated within the true species tree should replicate the observed mtDNA data. If mtDNA introgression has occurred, sequences simulated on alternative species trees, assuming closest relationships between the lineages showing highest mtDNA similarity, should better reproduce the observed data. Because the relationships between the

evolutionary lineages have not been resolved completely, both tests were based on four lineages with relationships well-supported by nuclear data: i) N *L. v. vulgaris*, *L. v. ampelensis*, *L. v. kosswigi* and *L. montandoni*; ii) S *L. v. vulgaris*, *L. v. meridionalis*, *L. v. schmidtleri* and *L. v. graecus* (Fig. 2). For *L. montandoni* two scenarios were evaluated, allowing introgression from either *L. v. ampelensis* or N *L. v. vulgaris*. For each evolutionary lineage we randomly sampled one sequence from each locality for which mtDNA sequences were available (Babik *et al.* 2005; Zieliński *et al.* 2013; Pabijan *et al.* 2015). These sequences were used to calculate parameters of competing species trees in BPP v3.1. A thousand gene trees were simulated for each species tree with MCcoal. Sequences were simulated along gene trees using SeqGen (Rambaut & Grass 1997) assuming the HKA + gamma model of sequence evolution with parameter values estimated in MEGA6 (Tamura *et al.* 2013). For each scenario mean and minimum uncorrected (p) distances between evolutionary lineages were calculated for 1000 simulated datasets and compared to the observed distances to obtain *P* values for individual comparisons. *P* values from individual tests were combined using Fisher's method.

Results

The largest dataset 1 contained 128 individuals and 74 loci with an average of 72.1 ± 20.29 haplotypes/locus (range 29-117) and 1.9 ± 3.87 % missing data per locus. Markers were of similar length (498.9 ± 6.79 bp) and highly polymorphic with an average of 91.8 ± 34.56 segregating sites per marker, one third of these (29.1 ± 9.52) were singleton polymorphisms (Table S4).

Species delimitation

Bayesian clustering solutions at $K \leq 6$ had low probabilities. Pr(K) plateaued at $K = 7$ (Fig. S2) and therefore we further only considered analyses at $K = 7$-12 (60 analyses in total). Most of these 60 analyses contained clusters that grouped all individuals of a given subspecies or

315 species together (Fig. 1B, Table S5). The top ten analyses with highest lnP all contained $K = 9$
316 groups with identical arrangements of individuals in clusters. Analyses with $K > 9$ contained
317 at least one cluster that was assigned zero or trivial fractions of the data, indicating that under
318 high K values, the number of meaningful clusters was lower than the assumed K. We thus
319 inferred 9 clusters with high certainty (Fig. 1B, Table S5). Five of these clusters correspond to
320 morphologically designated species or subspecies: *L. montandoni*, *L. v. graecus*, *L. v.*
321 *meridionalis*, *L. v. kosswigi* and *L. v. lantzi*. The nominative subspecies was subdivided into
322 two clusters that we designate North *L. v. vulgaris* (N *L. v. vulgaris*) and South *L. v. vulgaris*
323 (S *L. v. vulgaris*), with the former living predominantly to the north and east of the Carpathian
324 arc and the latter to the west and south of the Danube. The genetic cluster encompassing *L. v.*
325 *schmidtleri*, a subspecies described from western Anatolia that is morphologically similar to
326 the nominative subspecies, was also found in the southeastern Balkans. The genetic cluster
327 including *L. v. ampelensis* contained four individuals from eastern Slovakia, extreme western
328 Ukraine and Romania classified as *L. v. vulgaris* according to morphology. Following
329 Rosenberg *et al.* (2001), we consider that the frequency with which each taxon formed an
330 exclusive cluster over all 60 analyses is a good measure of its support (Table S5). This ranged
331 from 70% in *L. v. kosswigi* to 88% in *L. v. graecus* and *L. v. schmidtleri* and considerably
332 exceeded the frequency with which particular taxa clustered together or were split into two or
333 more groups. Some evidence of additional substructure was found in South *L. v. vulgaris* and
334 *L. v. graecus* (Fig. S3).

335 Admixture was consistently detected in nine individuals (7.0%; Fig. 1B, see Table S1
336 for estimated admixture proportions), five of which originated from the western part of the
337 range of *L. vulgaris* (admixed N *L. v. vulgaris*/S *L. v. vulgaris*, morphologically classified as
338 *L. v. vulgaris*), a single individual from northern Serbia (*L. v. ampelensis*/S *L. v. vulgaris*,
339 morphological *L. v. vulgaris*), one from Kosovo (S *L. v. vulgaris*/*L. v. graecus*,

morphologically undetermined), and two morphologically undetermined newts from the Romanian Carpathians composed of two (N *L. v. vulgaris*/*L. v. ampelensis*) or three (N *L. v. vulgaris*/*L. v. ampelensis*/*L. montandoni*) genetic clusters.

We conducted joint inference of species delimitation and phylogeny using BPP 3 with the 9 STRUCTURE-defined genetic clusters as OTUs. The posterior probabilities of each of these equaled 1.00 in all analyses under a wide range of priors and different starting trees (Table 1). All models in the 95% credibility sets contained the 9 putative species inferred from STRUCTURE.

We used the gene trees calculated in MrBayes to estimate the genealogical exclusivity of each candidate species. Typically, each genealogy in the post-burnin posteriors had a different topology. This was expected because there was limited phylogenetic information contained within each marker and many tips (257 including outgroup) in the trees. Unsurprisingly, consensus gene trees calculated for each marker were mostly unresolved, and showed high levels of discordance (data not shown). Nonetheless, the majority of the genealogies showed a nonrandom clustering pattern for the delimited *Lissotriton* groups as indicated by the highly significant *egsi* (Table 2). We inferred high exclusivity for *L. v. lantzi* and *L. v. kosswigi* with about 40% of genes monophyletic, and moderate *egsi* values for *L. v. graecus*, *L. v. schmidtleri*, *L. v. meridionalis* and *L. montandoni*. The values of *egsi* were relatively low but still highly significant for *L. v. ampelensis*, S *L. v. vulgaris* and N *L. v. vulgaris*.

Phylogenetic results

In concatenation analyses, we found that the individuals within STRUCTURE-defined genetic groups always formed clades with posterior probabilities (PP) of 1.0, we therefore collapsed individuals into groups and show a consensus tree over all replicates (Fig. 2A) and

364 separately for each of the 10 concatenation replicates (Fig. S4). The positions of some clades
365 were consistent across all replicates and were always fully supported (PP = 1.0). These
366 included the basal placement of *L. montandoni*, the subsequent split of a clade composed of *L.*
367 *v. graecus* and *L. v. kosswigi* and the sister group relationship of *L. v. meridionalis* and S *L. v.*
368 *vulgaris*. Moreover, the concatenated analyses invariably identified a fully supported clade
369 composed of *L. v. lantzi*, *L. v. schmidtleri*, S *L. v. vulgaris*, N *L. v. vulgaris*, *L. v. ampelensis*
370 and *L. v. meridionalis*. Our replicate analyses differed in the choice of sequences at
371 heterozygous loci during the concatenation process; the results show that this influenced the
372 branching patterns of the concatenated phylogenetic analyses by altering the positions of 4
373 taxa (N *L. v. vulgaris*, *L. v. schmidtleri*, *L. v. lantzi*, and *L. v. ampelensis*). Nearly all
374 alternative arrangements were strongly supported in one or more concatenation replicates
375 (Fig. S4).

376 A consensus of the 50 replicate primary concordance trees (Fig. 2B) shows that all *L.*
377 *vulgaris* taxa grouped together (to the exclusion of *L. montandoni*) across all replicates. The
378 mean concordance factor represented by the mean number of genes supporting this clade was
379 20.5 ± 2.2 out of a total of 70 genes. Other relatively well-supported clades include the sister
380 group relationship of *L. v. graecus* and *L. v. kosswigi*, as well as S *L. v. vulgaris* and *L. v.*
381 *meridionalis*, and a clade composed of *L. v. lantzi*, *L. v. schmidtleri*, N *L. v. vulgaris*, *L. v.*
382 *ampelensis*, S *L. v. vulgaris* and *L. v. meridionalis*. In each case concordance factors were low
383 (<10 genes with the exception of S *L. v. vulgaris* and *L. v. meridionalis*), suggesting that more
384 than one tree may equally well describe the history of these taxa. We examined this issue by
385 extracting concordance factors from each replicate BUCKy analysis for clades with relatively
386 high support (mostly encompassing those with two terminal taxa, Fig. S5). Primary histories
387 were well-discernible in the cases of *L. montandoni*, *L. v. meridionalis*, S *L. v. vulgaris*, *L. v.*
388 *lantzi*, *L. v. graecus* and *L. v. kosswigi*. However, between 3 and 6 primary histories could be

discerned for N *L. v. vulgaris*, *L. v. ampelensis* and *L. v. schmidtleri*, shown by similar mean concordance factors and largely overlapping quartiles (Fig. S5).

The multispecies coalescent model in BPP recovered a number of different species trees under the applied parameter settings (Table 1); their topologies and posterior probabilities varied depending on the prior specification, and to a limited extent, on seed number. Although the latter may suggest a lack of convergence, species trees with highest support were mostly consistent across analyses. Notably, *L. montandoni* and *L. v. ampelensis* were consistently recovered as sister taxa.

*BEAST was not an effective tool for analyzing the full dataset. For analyses based on 9 OTUs with 2 samples per taxon, parameter values converged for multiple runs of the same dataset and attained high effective sample sizes (all >200, most >1000). However, topological convergence was achieved in only 2 of 10 replicates, despite very similar likelihoods between replicate runs of the same dataset (Fig. S6). This suggests that the MCMCs became trapped on different peaks (i.e., different topologies) of high probability in independent runs. We attribute topological convergence problems to the large treespace involved in the analyses, and also to hybridization among taxa (see below). Furthermore, species tree topologies differed depending on the selected sequences (Fig. S6). In general, *L. v. graecus* and *L. v. kosswigi* were the most discrete in terms of node depth, while *L. montandoni* was consistently grouped with *L. v. ampelensis*, however, there was much uncertainty in clade heights and topology among taxa as shown by the scattered distribution of species trees in DensiTree plots (Fig. S6) and weakly supported summary trees. The only dense (but shallow) arrangement was found between S *L. v. vulgaris* and *L. v. meridionalis*.

Genetic divergence and haplotype sharing among OTUs

We found a gradient in divergence values (d_{xy}) among newt OTUs ranging between 1.14-1.59% (Fig. 3, Table S6). Each pair of taxa shared identical haplotypes at several loci (Fig. 3), with the highest proportions shared between N *L. v. vulgaris* and *L. v. ampelensis* (9.1%), *L. montandoni* and two other lineages (7.5 and 6.7% for N *L. v. vulgaris*-*L. montandoni* and *L. v. ampelensis*-*L. montandoni*, respectively) and three pairs involving S *L. v. vulgaris* and neighboring clades *L. v. ampelensis*, N *L. v. vulgaris* and *L. v. meridionalis* (5.2, 4.6 and 3.3%, respectively). All pairs involving the southern lineages shared few haplotypes (<3%). The slowly decaying tail starting at ca. 2% in the top panel of Figure 3 is probably indicative of the sharing of ancestral haplotypes.

Gene Flow among Taxa

The maximum likelihood topologies recovered by TreeMix based on 1 or 5 SNPs per marker (Fig. 2C) were very similar to the consensus topology of the concatenated analysis (Fig. 2A). After adding migration edges, we found a genetic contribution from *Lva* into *Lmon*, followed by gene flow of lesser magnitude from *Lvg* and *Lvs* into the ancestor of S*Lvv* and *Lvm* (Fig. 2D and Fig. S7). A fourth migration edge was inferred from *Lvk* into the outgroup, which we consider uninterpretable because the outgroup was composed of 3 different newt species.

In most pairwise taxon comparisons within the ABC framework at least one model could reproduce the observed data (Tables S7 and S8). The analyses had good power to discriminate between the four models (Table S8). Posterior probabilities for models varied considerably among pairwise taxa comparisons (Fig. 4A) with a clear predominance of the admixture (ADM) model and only 6 comparisons in which recent (in the last 200 kya) or continuous gene flow prevailed. However, in many cases episodes of gene flow in the ADM model were timed to have occurred deep in the past (e.g. modal values for posteriors >1 Ma), making ADM and NGF equivalent in the sense of ruling out recent and constant gene flow

(e.g. in *L. v. kosswigi-L. v. meridionalis*, *L. v. kosswigi-L. v. graecus*, *L. v. kosswigi-L. v. lantzi*, *L. montandoni-L. v. lantzi*, *L. montandoni*-S *L. v. vulgaris*; Table S9). In other cases modal values for admixture times in the ADM model were inferred to have occurred relatively recently, close to the upper limit of the prior (e.g. *L. montandoni-L. v. ampelensis*, N *L. v. vulgaris-L. v. kosswigi*), making the ADM and RGF models comparable. However, we note that posterior distributions for the admixture time parameters were in many cases very broad, indicating that data were not very informative in dating admixture events.

Phylogenies estimated from mtDNA under the assumption of ILS substantially differed from trees estimated assuming mtDNA introgression (i.e. the topology was incongruent with the species tree based on nuclear data, Fig. 5). Under ILS both entire trees and internal branches were very short. Minimum mtDNA divergence between lineages readily distinguished between ILS and hybridization. For both *L. montandoni* and *L. v. graecus*, scenarios assuming hybridization fit the data well and were strongly preferred over ILS (Table 3). One of the two hybridization scenarios involving *L. montandoni* fit the data better than the other, although both hybridization scenarios had much better fit than ILS. Apparently the scenario assuming introgression between N *L. v. vulgaris* and *L. montandoni* received higher support because of more extensive mtDNA haplotype sharing between these two than between *L. montandoni* and *L. v. ampelensis*. Mean mtDNA divergence between lineages was not informative in distinguishing between ILS and hybridization as both scenarios generated mean divergence that was not significantly different from the observed values (data not shown).

Discussion

This study documents a series of lineages representing a continuum of genetic divergence with evidence for contact between lineages and potential gene flow, which we interpret as a

speciation continuum in *Lissotriton* newts. We show that a combination of population genetic and phylogenetic approaches is required to describe and probe this transition. However, even the most sophisticated existing methods are not completely satisfactory because they do not incorporate all essential aspects of the process. For example, multispecies coalescent models assume that incomplete lineage sorting (ILS) is the only source of genealogical discordance, effectively ignoring hybridization, which is of major importance in the divergence of many taxa (Mallet 2005; Abbott *et al.* 2013; Harrison & Larson 2014). In the following sections we discuss our findings for *Lissotriton* newts, their more general implications and outline research areas where methodological advances are needed.

Robust delimitation despite substantial gene flow

All applied delimitation methods, based on allele frequencies, multispecies coalescent and genealogical concordance, robustly delimited nine evolutionary lineages. Some of these lineages correspond to described taxa, while others are morphologically cryptic (N *L. v. vulgaris*, S *L. v. vulgaris*) or include two distinct morphologies (*L. v. ampelensis*). This result is not an artifact of limited sampling under isolation by distance, because admixed individuals are rare and boundaries between lineages in well-sampled areas are sharp. The delimited entities are distinguishable in both allele frequency-based and genealogical frameworks, but are at various stages of divergence (Fig. 3). Substantial admixture between N *L. v. vulgaris* and S *L. v. vulgaris* in the postglacial expansion area in western Europe indicates that some lineages retain considerable potential for genetic exchange. We found evidence for recent gene flow between five other lineage pairs, confirming and extending previous work (Fig 4b; see Zieliński *et al*. 2016, for a detailed assessment of genetic exchange between *L. montandoni* and two *L. vulgaris* lineages). Moreover, episodes of gene flow between lineages in the more distant past may have been commonplace, given the overall weak support for the divergence with no gene flow model in the ABC analyses (Fig. 4), two cases of confirmed old

mtDNA introgression (Table 3), and several other instances of mtDNA paraphyly (Babik *et al.* 2005; Nadachowska & Babik 2009; Pabijan *et al.* 2015). Thus, it is by no means certain that all delimited newt lineages will continue to evolve independently. The newt system is a good example of a broader phenomenon: as reproductive isolation progresses, the incipient species experience a prolonged phase of parapatric/allopatric structured populations which may episodically exchange genes. This interpretation is in line with recent genetic and molecular studies of speciation showing that post-divergence gene flow is common, e.g. it was an important feature of hominin history (Pääbo 2015), and sometimes occurs at high levels (e.g. Nevado *et al.* 2011; Muir *et al.* 2012; Sun *et al.* 2012; Osborne *et al.* 2016).

Newt phylogeny and evolution of male nuptial morphology

The species tree of the *L. vulgaris* group could not be unequivocally resolved. Simulation studies indicate that multispecies coalescent-based species tree methods outperform concatenation even with a much smaller amount of genetic data, and can deal with substantial levels of incomplete lineage sorting (Ogilvie *et al.* 2016). In our case multispecies coalescent methods did not achieve topological convergence and most reconstructions produced by these methods were at odds with other evidence. The nontrivial amount of reticulate evolution among Central European newt taxa is likely the reason for the poor performance of *BEAST and species tree estimation in BPP, because it violates their assumption that all discordance is due to ILS. It has been shown in simulations that gene flow between nonsister taxa leads to erroneous inference in species tree methods (Leaché *et al.* 2014; Solís-Lemus *et al.* 2016). In our analyses, conflicting evidence from various loci caused by mixing signals of introgression and ILS leads to multiple peaks in the posterior distributions of species trees and a lack of topological convergence. In this context, the concatenation and concordance analyses that we applied were more compatible with the TreeMix results that specifically incorporate reticulation, and hence more reliable in inferring the species tree in the presence of gene flow

among OTUs. Given the increasing number of studies reporting reticulate evolution, there is an urgent need for progress in methods co-estimating phylogeny and gene flow in multispecies and multilocus datasets; phylogenetic multilocus network methods (Yu *et al.* 2013; 2014; Solís-Lemus & Ané 2016) appear promising in this respect.

The partially resolved species tree for the *L. vulgaris* group nonetheless sheds light on morphological evolution. The male nuptial morphology of *L. montandoni* consists of a smooth and low crest, prominent tail filament and dorso-lateral ridges. Similar male morphologies are also present in the more distantly related *L. helveticus*, *L. italicus* and *L. boscai*. This particular suite of phenotypic traits may be an adaptation for the effective transmission of waterborne pheromones (Pecio & Rafiński 1985) and could signify the predominance of olfactory cues for species recognition in these newts (Secondi *et al.* 2005). On the other hand, the derived condition of prominent crests and overall larger male body size in most *L. vulgaris* lineages indicates a shift towards visual cues (Secondi *et al.* 2012), although other explanations are possible such as divergence in female preference for larger male body size (Haerty *et al.* 2007; Secondi *et al.* 2010). Whatever the underlying cause(s), our species phylogeny shows that *montandoni*-like male morphology was present in the ancestral *L. vulgaris* population, conserved in the *L. v. kosswigi*/*L. v. graecus* clade, and replaced by the derived morphology in the sister clade giving rise to other extant *L. vulgaris* lineages. The intermediate breeding male morphologies of *L. v. ampelensis* and *L. v. meridionalis* (Raxworthy 1990) could be interpreted as independent, partial reversions to the ancestral morphology due to convergent evolution. Alternatively, and possibly more likely given the evidence for substantial gene flow from neighboring taxa, these intermediate morphologies could be the result of an influx of genes underlying the derived morphology and dilution of *montandoni*-like ancestral traits. These two hypotheses could be tested with genome-wide data.

Isolation and gene flow revealed by ABC modeling

Recognizing the limitations of existing methodologies, we explored gene flow between pairs of taxa in a model-based framework using Approximate Bayesian Computation (ABC). This approach, although quite simple, has been effective in unraveling the process of gene flow in the newt system. The data had good power in distinguishing among the four scenarios of gene flow and provided quantitative measures of support for the various models. However, analyses modeling gene flow between two populations without incorporation of additional populations have been criticized because ignoring such "ghost" populations may affect parameter estimates or even model choice (Beerli 2004; Slatkin 2005; Strasburg & Rieseberg 2010; Eaton *et al.* 2015). We note though that pairwise comparisons among all extant taxa may partially alleviate this issue. The availability of all pairwise comparisons allows the identification and reinterpretation of problematic cases, such as support for recent gene flow between allopatric taxa which have not likely been in recent contact, but which both may have exchanged genes with other populations. In our case, inferences were largely consistent with geographic distributions of the lineages and we accept them as working hypotheses. In general, given the current state of the field, the use of simple pairwise models in complexes of interbreeding species may be useful because they offer a feasible way of distinguishing among different scenarios of gene flow and building more complex, but still testable, hypotheses.

In addition to model selection, ABC estimates demographic parameters which facilitate the interpretation of evolutionary history along the speciation continuum. Estimates of long-term, coalescent effective population sizes (N_e) for the *Lissotriton* lineages are quite large, ranging roughly between 80,000 and 800,000 (Table S9). Independent assessments place the divergence time of *L. montandoni* and *L. vulgaris* between 3.7 to 6.3 mya (Stuglik & Babik 2016), while mtDNA lineages within *L. vulgaris* split in close succession during the

late Pliocene and Pleistocene (Babik *et al*. 2005; Pabijan *et al*. 2015). This timeframe suggests that most *Lissotriton* lineages have not attained the $4N_e$ generations when roughly half of the loci in the genome achieve reciprocal monophyly (Hudson & Coyne 2002; Degnan & Rosenberg 2009), thus widespread incomplete lineage sorting (Table 2) and the presence of identical haplotypes amongst all lineage pairs are expected (Fig. 3). However, the lineages exchanging genes most extensively (*L. v. ampelensis*, N *L. v. vulgaris*, S *L. v. vulgaris*, *L. v. meridionalis*) also have the largest N_e's (Fig. 4B, Table S9). This suggests that post-divergence gene flow contributed to elevated N_e estimates, although long-term population structure within lineages may also inflate N_e. We postulate that the existence of a transitional phase, in which differentiated lineages exchange genes, may explain or contribute to the large ancestral population sizes inferred by various methods (IM, ABC, PSMC) in many species (e.g. Won *et al.* 2005; Duvaux *et al.* 2011; Nadachowska-Brzyska *et al.* 2015).

One potentially important consequence of limited but persistent gene flow among a set of parapatrically distributed and non-reproductively isolated taxa is the opportunity for adaptive introgression. The flow of fitness-increasing genetic variants across species boundaries is a source of genetic and phenotypic variation and may increase rates of adaptive change in recipient species (Rieseberg *et al*. 2004; Hedrick 2013; Racimo *et al.* 2015). In divergent species, the parts of the genome most prone to genetic exchange may be those underlying phenotypic variation in systems challenged by new environments such as the skin and the immune system. There is tentative evidence for adaptive introgression of MHC class II genes between *L. montandoni* and several central European *L. vulgaris* lineages (Nadachowska-Brzyska *et al*. 2012). Thus, the overall pattern of genetic integrity in *L. montandoni* is breached by the interspecies transfer of neutral and putatively adaptive alleles. We suggest that the speciation continuum in *Lissotriton* newts documented herein may

provide a suitable system with multiple replicates to study the significance of introgression of adaptive variants from other species.

Introgression explains mtDNA paraphyly

With a partially resolved phylogeny, we were able to test statistically for mtDNA introgression suggested previously. We confirmed introgression in two of the most striking cases (from N *L. v. vulgaris* into *L. montandoni* and S *L. v. vulgaris* into *L. v. graecus*), effectively explaining the discordance between mtDNA, nuclear genes and morphology, and attributing it to extensive recent and ancient mtDNA introgression. While there is evidence that it has been accompanied by introgression of nuclear genes in the case of *L. montandoni*, we do not have strong evidence of nuclear introgression into *L. v. graecus*. Better power to reconstruct the extent and timing of nuclear introgression would be obtained with a larger amount of data, particularly from longer genomic regions to explore information contained in haplotype spectra (Harris & Nielsen 2013).

Taxonomic Implications

We note that the application of a rigid taxonomy in which we appropriate scientific names to all nine genetically distinct lineages delimited herein would not fully capture the intricacies of the evolutionary history of *Lissotriton* newts. As stated previously (Wiens 2007), the delimitation of species poses the problem of thresholding the continuous processes of speciation and lineage amalgamation. Although a number of authors have recognized some of the morphological *L. vulgaris* subspecies as full species (e.g. Dubois & Raffaëlli 2009; Skorinov *et al.* 2014; Wielstra *et al.* 2015; Frost 2016), these relegations were not based on new data but on inconclusive mtDNA variation, geographic range limits, and morphology.

We delimited three distinct southern taxa for which our data strongly suggest species status: *L. v. graecus* as *L. graecus* (Wolterstorff, 1906), *L. v. kosswigi* as *L. kosswigi* (Freytag, 1955), and *L. v. lantzi* as *L. lantzi* (Wolterstorff, 1914). We base this assertion on the concordant signals of divergence and independence from allele frequency- and genealogy-based delimitation methods, genealogical sorting, a nearly complete lack of hybrids in well-sampled areas and little evidence for genetic exchange in the recent past. Moreover, *L. lantzi* and *L. kosswigi* are allopatrically distributed (Skorinov *et al.* 2014; Wielstra *et al.* 2015), making gene exchange with other lineages improbable in the near future. On the other hand, four central European *L. vulgaris* lineages are interconnected by nontrivial amounts of gene flow. These taxa show fusion following range expansion in the morphologically cryptic N *L. v. vulgaris* and S *L. v. vulgaris*, extensive genetic exchange with neighboring lineages in *L. v. ampelensis*, and continuous gene flow since divergence between *L. v. meridionalis* and S *L. v. vulgaris*. These results suggest that we may be observing the loss of incipient divergence through hybridization in these taxa. Finally, although *L. v. schmidtleri* [and not *L. schmidtlerorum*, see Dubois (2007) and Dubois & Raffaëlli (2009)] is recovered as distinct in our analyses, we refrain from making a taxonomic judgment on this lineage pending more extensive sampling in northeastern Bulgaria and southern Romania, which may constitute a contact zone between several smooth newt lineages.

Conclusions

We found that *Lissotriton* newts represent a continuum of genetic divergence with varying levels of shared genetic variation among taxon pairs. This pattern invokes long-term isolation and independent evolution in three southern smooth newt species, genetic exchange across parapatric borders for several taxa in Central Europe, and effective fusion of previously separated gene pools of two lineages in the post-glacial expansion areas of Western Europe. The profound discordance between taxonomic boundaries and mtDNA in *Lissotriton* is

631 explained by extensive mtDNA introgression rather than by other processes. These features
632 make the *L. vulgaris* species group a suitable system to examine the fission/fusion dynamics
633 of the speciation continuum. The newt system is relevant because many species may have
634 experienced such long-term structured populations. However, we also highlight that better
635 methods, jointly modeling incomplete lineage sorting and gene flow, are needed to analyze
636 such systems.

637 Acknowledgments

638 We thank Marcin Piwczyński and Ben Wielstra for insightful comments on the manuscript.
639 Piotr Grodek, Marcin Liana and Krystyna Nadachowska-Brzyska offered invaluable help in
640 the field. Pim Arntzen, Konstantinos Sotiropoulos and Ben Wielstra generously shared
641 samples and locality information. The work was funded by the Polish National Science Centre
642 (2012/04/A/NZ8/00662 to W.B) and the Jagiellonian University (DS/WBiNoZ/INoS/762/15).

643

References

Abbott R, Albach D, Ansell S, Arntzen JW, Baird SJ, Bierne N, Boughman J, Brelsford A, Buerkle CA, Buggs R, Butlin RK, Dieckmann U, Eroukhmanoff F, Grill A, Cahan SH, Hermansen JS, Hewitt G, Hudson AG, Jiggins C, Jones J, Keller B, Marczewski T, Mallet J, Martinez-Rodriguez P, Möst M, Mullen S, Nichols R, Nolte AW, Parisod C, Pfennig K, Rice AM, Ritchie MG, Seifert B, Smadja CM, Stelkens R, Szymura JM, Väinölä R, Wolf JB, Zinner D (2013) Hybridization and speciation. *Journal of Evolutionary Biology*, **26**, 229–246.

Ané C, Larget B, Baum DA, Smith SD, Rokas A (2007) Bayesian estimation of concordance among gene trees. *Molecular Biology & Evolution*, **24**, 412–426.

Babik W, Rafiński J (2004) Relationship between morphometric and genetic variation in pure and hybrid populations of the smooth and Montandon's newt (*Triturus vulgaris* and *T. montandoni*). *Journal of Zoology*, **262**, 135–143.

Babik W, Szymura JM, Rafiński J (2003) Nuclear markers, mitochondrial DNA and male secondary sexual traits variation in a newt hybrid zone (*Triturus vulgaris*×*T. montandoni*). *Molecular Ecology*, **12**, 1913–1930.

Babik W, Branicki W, Crnobrnja-Isailović J, Cogălniceanu D, Sas I, Olgun K, Poyarkov NA, Garcia-París M, Arntzen JW (2005) Phylogeography of two European newt species—discordance between mtDNA and morphology. *Molecular Ecology*, **14**, 2475–2491.

Beerli P (2004) Effect of unsampled populations on the estimation of population sizes and migration rates between sampled populations. *Molecular Ecology*, **13**, 827–836.

Bouckaert RR (2010) DensiTree: making sense of sets of phylogenetic trees. *Bioinformatics*, **26**, 1372–1373.

Bouckaert R, Heled J, Kühnert D, Vaughan T, Wu CH, Xie D, Suchard MA, Rambaut A, Drummond AJ (2014) BEAST 2: a software platform for Bayesian evolutionary analysis. *PLoS Computational Biology*, **10**, e1003537.

Bour R, Bringsøe H, Vanderhaege M (2002) *Triturus vulgaris* (Linnaeus, 1758) at its southern limit: distribution on the Peloponnese, Greece, with range extensions from the Central and South Peloponnese. *Alytes*, **20**, 67–76.

Bousbouras D, Ioannidis Y (1997) The distribution and habitat preferences of the amphibians of Prespa National Park. In: *Lake Prespa, Northwestern Greece. A Unique Balkan Wetland* (eds. Crivelli AJ, Catsadorakis G), pp. 127–133. Springer, the Netherlands.

Coyne JA, Orr HA (2004) *Speciation*. Sinauer Associates, Sunderland, MA.

Cruickshank TE, Hahn MW (2014) Reanalysis suggests that genomic islands of speciation are due to reduced diversity, not reduced gene flow. *Molecular Ecology*, **23**, 3133–3157.

Cummings MP, Neel MC, Shaw KL (2008) A genealogical approach to quantifying lineage divergence. *Evolution*, **62**, 2411–2422.

Darriba D, Taboada GL, Doallo R, Posada D (2012) jModelTest 2: more models, new heuristics and parallel computing. *Nature Methods*, **9**, 772.

Degnan JH, Rosenberg NA (2009) Gene tree discordance, phylogenetic inference and the multispecies coalescent. *Trends in Ecology & Evolution*, **24**, 332–340.

de Queiroz K (2007) Species concepts and species delimitation. *Systematic Biology*, **56**, 879–886.

Dubois A (2007) Genitives of species and subspecies nomina derived from personal names should not be emended. *Zootaxa*, **1550**, 49–68.

Dubois A, Raffaëlli J (2009) A new ergotaxonomy of the family Salamandridae Goldfuss, 1820 (Amphibia, Urodela). *Alytes*, **26**, 1–85.

Duvaux L, Belkhir K, Boulesteix M, Boursot P (2011) Isolation and gene flow: inferring the speciation history of European house mice. *Molecular Ecology*, **20**, 5248–5264.

Earl DA, vonHoldt BM (2012) STRUCTURE HARVESTER: a website and program for visualizing STRUCTURE output and implementing the Evanno method. *Conservation Genetics Resources*, **4**, 359–361.

Eaton DA, Hipp AL, González-Rodríguez A, Cavender-Bares J (2015) Historical introgression among the American live oaks and the comparative nature of tests for introgression. *Evolution*, **69**, 2587–2601.

Excoffier L, Dupanloup I, Huerta-Sánchez E, Sousa VC, Foll M (2013) Robust demographic inference from genomic and SNP data. *PLoS Genetics*, **9**, e1003905.

Frost D.R. 2016. Amphibian Species of the World 6.0, an Online reference. http://research.amnh.org/vz/herpetology/amphibia/ (accessed on 20/12/2016)

Harris K, Nielsen R (2013) Inferring demographic history from a spectrum of shared haplotype lengths. *PLoS Genetics*, **9**, e1003521.

Harrison RG, Larson EL (2014) Hybridization, introgression, and the nature of species boundaries. *Journal of Heredity*, **105**, 795–809.

Haerty W, Gentilhomme E, Secondi J (2007) Female preference for a male sexual trait uncorrelated with male

body size in the palmate newt (*Triturus helveticus*). *Behaviour*, **144**, 797–814.
Hedrick PW (2013) Adaptive introgression in animals: examples and comparison to new mutation and standing variation as sources of adaptive variation. *Molecular Ecology*, **22**, 4606–4618.
Heled J, Drummond AJ (2010) Bayesian inference of species trees from multilocus data. *Molecular Biology & Evolution*, **27**, 570–580.
Huang J-P, Knowles LL (2016) The species versus subspecies conundrum: quantitative delimitation from integrating multiple data types within a single Bayesian approach in Hercules beetles. *Systematic Biology*, **65**, 685–699.
Hudson RR, Coyne JA (2002) Mathematical consequences of the genealogical species concept. *Evolution*, **56**, 1557–1565.
Joyce DA, Lunt DH, Genner MJ, Turner GF, Bills R, Seehausen O (2011). Repeated colonization and hybridization in Lake Malawi cichlids. *Current Biology*, **21**, R108–R109.
Kotlík P, Zavadil V (1999) Natural hybrids between the newts *Triturus montandoni* and *T. vulgaris*: morphological and allozyme data evidence of recombination between parental genomes. *Folia Zoologica*, **48**, 211–218.
Kopelman NM, Mayzel J, Jakobsson M, Rosenberg NA, Mayrose I (2015) Clumpak: a program for identifying clustering modes and packaging population structure inferences across K. *Molecular Ecology Resources*, **15**, 1179–1191.
Krizmanic I, Mesaroš G, Džukic G, Kalezic ML (1997) Morphology of the smooth newt (*Triturus vulgaris*) in former Yugoslavia: taxonomical implications and distribution patterns. *Acta Zoologica Academiae Scientiarum Hungaricae*, **43**, 345–357.
Larget B, Kotha SK, Dewey CN, Ané C (2010) BUCKy: Gene tree / species tree reconciliation with the Bayesian concordance analysis. *Bioinformatics*, **26**, 2910–2911.
Leaché AD, Harris RB, Rannala B, Yang Z (2014) The influence of gene flow on species tree estimation: a simulation study. *Systematic Biology*, **63**, 17–30.
Leuenberger C, Wegmann D (2010) Bayesian computation and model selection without likelihoods. *Genetics*, **184,** 243–252.
Librado P, Rozas J (2009) DnaSP v5: A software for comprehensive analysis of DNA polymorphism data. *Bioinformatics*, **25**, 1451–1452.
Macgregor HC, Sessions SK, Arntzen JW (1990) An integrative analysis of phylogenetic relationships among newts of the genus *Triturus* (family Salamandridae), using comparative biochemistry, cytogenetics and reproductive interactions. *Journal of Evolutionary Biology*, **3**, 329–373.
Mallet J (2005) Hybridization as an invasion of the genome. *Trends in Ecology and Evolution*, **20**, 229–237.
Michalak P, Rafiński J (1999) Sexual isolation between two newt species, *Triturus vulgaris* and *T. montandoni* (Amphibia, Urodela, Salamandridae). *Biological Journal of the Linnean Society*, **67**, 343–352.
Michalak P, Grzesik J, Rafiński J (1997) Tests for sexual incompatibility between two newt species, *Triturus vulgaris* and *Triturus montandoni*: no-choice mating design. *Evolution*, **51**, 2045–2050.
Miller MA, Pfeiffer W, Schwartz T (2010) Creating the CIPRES Science Gateway for inference of large phylogenetic trees. *Proceedings of the Gateway Computing Environments Workshop (GCE)*, 1–8.
Muir G, Dixon CJ, Harper AL, Filatov DA (2012) Dynamics of drift, gene flow, and selection during speciation in *Silene*. *Evolution*, **66**, 1447–1458.
Nadachowska K, Babik W (2009) Divergence in the face of gene flow: the case of two newts (Amphibia: Salamandridae). *Molecular Biology & Evolution*, **26**, 829–841.
Nadachowska-Brzyska K, Zieliński P, Radwan J, Babik W (2012) Interspecific hybridization increases MHC class II diversity in two sister species of newts. *Molecular Ecology*, **21**, 887–906.
Nadachowska-Brzyska K, Li C, Smeds L, Zhang G, Ellegren H (2015) Temporal dynamics of avian populations during Pleistocene revealed by whole-genome sequences. *Current Biology*, **25**, 1375–1380.
Nevado B, Fazalova V, Backeljau T, Hanssens M, Verheyen E (2011) Repeated unidirectional introgression of nuclear and mitochondrial DNA between four congeneric Tanganyikan cichlids. *Molecular Biology & Evolution*, **28**, 2253–2267.
Nylander JA, Wilgenbusch JC, Warren DL, Swofford DL (2008) AWTY (are we there yet?): a system for graphical exploration of MCMC convergence in Bayesian phylogenetics. *Bioinformatics*, **24**, 581–583.
Ogilvie HA, Heled J, Xie D, Drummond AJ (2016) Computational performance and statistical accuracy of *BEAST and comparisons with other methods. *Systematic Biology*, **65**, 381–396.
Osborne O, Chapman M, Nevado B, Filatov D (2016) Maintenance of species boundaries despite ongoing gene flow in ragworts. *Genome Biology & Evolution*, **8**, 1038–1047.
Pabijan M, Zieliński P, Dudek K, Chloupek M, Sotiropoulos K, Liana M, Babik W (2015) The dissection of a Pleistocene refugium: phylogeography of the smooth newt, *Lissotriton vulgaris*, in the Balkans. *Journal of Biogeography*, **42**, 671–683.
Pääbo S (2015) The diverse origins of the human gene pool. *Nature Reviews Genetics*, **16**, 313–314.

762 Pecio A, Rafiński J (1985) Sexual behaviour of the Montandon's newt, *Triturus montandoni*
763 (Boulenger)(Caudata: Salamandridae). *Amphibia-Reptilia*, **6**, 11–22.
764 Petit RJ, Excoffier L (2009) Gene flow and species delimitation. *Trends in Ecology & Evolution*, **24**, 386–393.
765 Pickrell JK, Pritchard JK (2012) Inference of population splits and mixtures from genome-wide allele frequency
766 data. *PLoS Genetics*, **8**, e1002967.
767 Pritchard JK, Stephens M, Donnelly P (2000) Inference of population structure using multilocus genotype data.
768 *Genetics*, **155**, 945–959.
769 Racimo F, Sankararaman S, Nielsen R, Huerta-Sánchez E (2015) Evidence for archaic adaptive introgression in
770 humans. *Nature Reviews Genetics*, **16**, 359–371.
771 Rafiński J, Arntzen JW (1987) Biochemical systematics of the Old World newts, genus *Triturus*: allozyme data.
772 *Herpetologica*, **43**, 446–457.
773 Rambaut A, Drummond AJ (2007) Tracer v1. 5. http://*tree.bio.ed.ac.uk/software/tracer*
774 Rambaut A, Grass NC (1997) Seq-Gen: an application for the Monte Carlo simulation of DNA sequence
775 evolution along phylogenetic trees. *Computer Applications in the Biosciences*, **13**, 235–238.
776 Rannala B, Yang Z (2013) Improved reversible jump algorithms for Bayesian species delimitation. *Genetics*,
777 **194**, 245–253.
778 Raxworthy CJ (1990) A review of the smooth newt (*Triturus vulgaris*) subspecies, including an identification
779 key. *Herpetological Journal*, **1**, 481–492.
780 Rieseberg LH, Burke JM (2001) The biological reality of species: gene flow, selection, and collective evolution.
781 *Taxon*, **50**, 47–67.
782 Rieseberg LH, Church SA, Morjan CL (2004) Integration of populations and differentiation of species. *New*
783 *Phytologist*, **161**, 59–69.
784 Rhymer JM, Simberloff D (1996) Extinction by hybridization and introgression. *Annual Review in Ecology &*
785 *Systematics*, **27**, 83–109.
786 Ronquist F, Teslenko M, van der Mark P, Ayres DL, Darling A, Höhna S, Larget B, Liu L, Suchard MA,
787 Huelsenbeck JP (2012) MrBayes 3.2: efficient Bayesian phylogenetic inference and model choice across a
788 large model space. *Systematic Biology*, **61**, 539–542.
789 Rosenberg NA, Burke T, Elo K, Feldman MW, Freidlin PJ, Groenen MAM, Hillel J, Mäki-Tanila A, Tixier-
790 Boichard M, Vignal A, Wimmers K, Weigend S (20010 Empirical evaluation of genetic clustering methods
791 using multilocus genotypes from 20 chicken breeds. *Genetics*, **159**, 699–713.
792 Rudman SM, Schluter D (2016) Ecological impacts of reverse speciation in threespine stickleback. *Current*
793 Biology, **26**, 490–495.
794 Schmidtler JF, Franzen M (2004) *Triturus vulgaris* (Linnaeus, 1758)–Teichmolch. In: *Handbuch der Reptilien*
795 *und Amphibien Europas* (eds. Grossenbacher K., Thiesemeier B.), pp. 847–967. Aula Verlag, Wiesbaden,
796 Germany.
797 Schmidtler JJ, Schmidtler JF (1983) Verbreitung, Ökologie und unterartliche Gliederung von *Triturus vulgaris*
798 in der adriatischen Küstengebieten (Amphibia, Salamandridae). *Spixiana*, **6**, 229–249.
799 Secondi J, Haerty W, Lodé T (2005) Female attraction to conspecific chemical cues in the palmate newt *Triturus*
800 *helveticus*. *Ethology*, **111**, 726–735.
801 Secondi J, Johanet A, Pays , Cazimajou F, Djalout Z, Lemaire C (2010) Olfactory and visual species recognition
802 in newts and their role in hybridization. *Behaviour*, **147**, 1693–1712.
803 Secondi J, Lepetz V, Théry M (2012) Male attractiveness is influenced by UV wavelengths in a newt species but
804 not in its close relative. *PLoS One*, **7**, e30391.
805 Skorinov DV, Kuranova VN, Borkin LJ, Litvinchuk SN (2008) Distribution and conservation status of the
806 Smooth Newt (*Lissotriton vulgaris*) in Western Siberia and Kazakhstan. *Russian Journal of Herpetology*, **15**,
807 157–165.
808 Skorinov D, Doronin I, Kidov A, Tuniev B, Litvinchuk S (2014) Distribution and conservation status of the
809 Caucasian newt, *Lissotriton lantzi* (Wolterstorff, 1914). *Russian Journal of Herpetology*, **21**, 251–268.
810 Slatkin M (1985) Gene flow in natural populations. *Annual Review in Ecology & Systematics*, **16**, 393–430.
811 Slatkin M (2005) Seeing ghosts: the effect of unsapled populations on migration rates estimated for sampled
812 populations. *Molecular Ecology*, **14**, 67–73.
813 Solís-Lemus C, Ané C (2016) Inferring phylogenetic networks with maximum pseudolikelihood under
814 incomplete lineage sorting. *PLoS Genetics*, **12**, e1005896.
815 Solís-Lemus C, Yang M, Ané C (2016) Inconsistency of species-tree methods under gene flow. *Systematic*
816 *Biology*, available online, doi: 10.1093/sysbio/syw030.
817 Sousa V, Hey J (2013) Understanding the origin of species with genome-scale data: modelling gene flow. *Nature*
818 *Reviews Genetics*, **14**, 404–414.
819 Speybroeck J, Beukema W, Crochet P-A (2010) A tentative species list of the European herpetofauna
820 (Amphibia and Reptilia)–an update. *Zootaxa*, **2492**, 1–27.
821 Strasburg JL, Rieseberg LH (2010) How robust are “isolation with migration” analyses to violations of the IM

model? A simulation study. *Molecular Biology & Evolution*, **27**, 297–310.
Stuglik MT, Babik W (2016) Genomic heterogeneity of historical gene flow between two species of newts inferred from transcriptome data. *Ecology & Evolution*, **6**, 4513–4525.
Sun Y, Corcoran P, Menkis A, Whittle CA, Andersson SG, Johannesson H (2012) Large-scale introgression shapes the evolution of the mating-type chromosomes of the filamentous ascomycete *Neurospora tetrasperma*. *PLoS Genetics*, **8**, e1002820.
Tamura K, Stecher G, Peterson D, Filipski A, Kumar S (2013) MEGA6: molecular evolutionary genetics analysis version 6.0. *Molecular Biology & Evolution*, **30**, 2725–2729.
Wegmann D, Leuenberger C, Neuenschwander S, Excoffier L (2010) ABCtoolbox: a versatile toolkit for approximate Bayesian computations. *BMC Bioinformatics*, **11**, 116.
Wielstra B, Bozkurt E, Olgun K (2015) The distribution and taxonomy of *Lissotriton* newts in Turkey (Amphibia, Salamandridae). *ZooKeys*, **484**, 11–23.
Wiens JJ (2007) Species delimitation: new approaches for discovering diversity. *Systematic Biology*, **56**, 875–878.
Weisrock DW, Smith SD, Chan LM, Biebouw K, Kappeler PM, Yoder AD (2012) Concatenation and concordance in the reconstruction of mouse lemur phylogeny: an empirical demonstration of the effect of allele sampling in phylogenetics. *Molecular Biology & Evolution*, **29**, 1615–1630.
Wolf JB, Ellegren H (2016) Making sense of genomic islands of differentiation in light of speciation. *Nature Reviews Genetics*, available online, doi:10.1038/nrg.2016.133
Won YJ, Sivasundar A, Wang Y, Hey J (2005) On the origin of Lake Malawi cichlid species: a population genetic analysis of divergence. *Proceedings of the National Academy of Sciences*, **102**, 6581–6586.
Yang Z (2015) The BPP program for species tree estimation and species delimitation. *Current Zoology*, **61**, 854–865.
Yang Z, Rannala B (2010) Bayesian species delimitation using multilocus sequence data. *Proceedings of the National Academy of Sciences*, **107**, 9264–9269.
Yang Z, Rannala B (2014) Unguided species delimitation using DNA sequence data from multiple loci. *Molecular Biology & Evolution*, **31**, 3125–3135.
Yu Y, Barnett RM, Nakhleh L (2013) Parsimonious inference of hybridization in the presence of incomplete lineage sorting. *Systematic Biology*, **62**, 738–751.
Yu Y, Dong J, Liu KJ, Nakhleh L (2014) Maximum likelihood inference of reticulate evolutionary histories. *Proceedings of the National Academy of Sciences*, **111**, 16448–16453.
Zieliński P, Nadachowska-Brzyska K, Wielstra B, Szkotak R, Covaciu-Marcov SD, Cogălniceanu D, Babik W (2013) No evidence for nuclear introgression despite complete mtDNA replacement in the Carpathian newt (*Lissotriton montandoni*). *Molecular Ecology*, **22**, 1884–1903.
Zieliński P, Stuglik MT, Dudek K, Konczal M, Babik W (2014) Development, validation and high-throughput analysis of sequence markers in nonmodel species. *Molecular Ecology Resources*, **14**, 352–360.
Zieliński P, Nadachowska-Brzyska K, Dudek K, and Babik W (2016) Divergence history of the Carpathian and smooth newts modelled in space and time. *Molecular Ecology*, **25**, 3912–3928.

Data accessibility

Input data and scripts used for data transformation and analysis are available in Dryad digital repository with doi:[to be submitted upon manuscript acceptance]. DNA sequence alignments for all markers were submitted to GenBank: accession nos. [to be submitted upon manuscript acceptance]. Additional analyses are provided as Supporting Information.

867 ## Author Contributions

868 MP and WB designed the research, analyzed the data and wrote the paper. KD and MP
869 conducted laboratory analyses. PZ and MS contributed analytical tools and helped analyze the
870 data. All authors approved of a final version of the manuscript.

871

872 **Table 1**. Joint Bayesian species delimitation and species tree estimation in the *Lissotriton*
873 *vulgaris* species group using BPP. Rows show results for different analyses; letters denote
874 replicate runs differing only by seed number. Population size (θ) and divergence time (τ)
875 priors encompass a wide range of demographic and divergence scenarios. Starting guide tree
876 topologies were random unless specified otherwise (see footnotes). *N* species shows the
877 numbers of species and their posterior probabilities (PPs) in each analysis (PPs for each
878 species within analyses were always 1.00). *N* trees denotes the number of trees in the 95%
879 credibility set, and the last column shows the topology and posterior probability of the highest
880 ranked tree in the set.

Runs	Θ[a]	τ[a]	*N* species (PP)	*N* trees	best tree and pp of model (delimitation + tree)
1a	G(1, 35)	G(2, 500)	9 (1.00)	7	(*L. v. graecus*, (*L. v. lantzi*, ((*L. v. schmidtleri*, *L. v. kosswigi*), ((S *L. v. vulgaris*, *L. v. meridionalis*), (N *L. v. vulgaris*, (*L. montandoni*, *L. v. ampelensis*)))))); 0.70905
1b	G(1, 35)	G(2, 500)	9 (1.00)	4	(*L. v. graecus*, (*L. v. lantzi*, (*L. v. kosswigi*, ((S *L. v. vulgaris*, *L. v. meridionalis*), (*L. v. schmidtleri*, (N *L. v. vulgaris*, (*L. montandoni*, *L. v. ampelensis*)))))); 0.83335
2a[b]	G(1, 35)	G(2, 500)	9 (1.00)	4	(*L. v. graecus*, (*L. v. lantzi*, (*L. v. kosswigi*, ((S *L. v. vulgaris*, *L. v. meridionalis*), (*L. v. schmidtleri*, (N *L. v. vulgaris*, (*L. montandoni*, *L. v. ampelensis*)))))); 0.81770
2b[b]	G(1, 35)	G(2, 500)	9 (1.00)	2	(*L. v. graecus*, (*L. v. lantzi*, (*L. v. kosswigi*, ((S *L. v. vulgaris*, *L. v. meridionalis*), (*L. v. schmidtleri*, (N *L. v. vulgaris*, (*L. montandoni*, *L. v. ampelensis*)))))); 0.88070
3a[c]	G(1, 35)	G(2, 500)	9 (1.00)	3	(*L. v. graecus*, (*L. v. lantzi*, (*L. v. kosswigi*, ((S *L. v. vulgaris*, *L. v. meridionalis*), (*L. v. schmidtleri*, (N *L. v. vulgaris*, (*L. montandoni*, *L. v. ampelensis*)))))); 0.82170
3b[c]	G(1, 35)	G(2, 500)	9 (1.00)	2	(*L. v. graecus*, (*L. v. lantzi*, (*L. v. kosswigi*, ((S *L. v. vulgaris*, *L. v. meridionalis*), (*L. v. schmidtleri*, (N *L. v. vulgaris*, (*L. montandoni*, *L. v. ampelensis*)))))); 0.85825
4a[d]	G(1, 35)	G(2, 500)	9 (1.00)	3	(*L. v. graecus*, (*L. v. lantzi*, (*L. v. kosswigi*, ((S *L. v. vulgaris*, *L. v. meridionalis*), (*L. v. schmidtleri*, (N *L. v. vulgaris*, (*L. montandoni*, *L. v. ampelensis*)))))); 0.79815
4b[d]	G(1, 35)	G(2, 500)	9 (1.00)	38	(*L. v. graecus*, (*L. v. lantzi*, (*L. v. kosswigi*, ((S *L. v. vulgaris*, *L. v. meridionalis*), (*L. v. schmidtleri*, (N *L. v. vulgaris*, (*L. montandoni*, *L. v. ampelensis*)))))); 0.43710
5a	G(1, 10)	G(2, 2000)	9 (1.00)	9	(*L. v. graecus*, (*L. v. lantzi*, (*L. v. kosswigi*, (*L. v. meridionalis*, (*L. v. schmidtleri*, ((*L. montandoni*, *L. v. ampelensis*), (N *L. v. vulgaris*, S *L. v. vulgaris*)))))); 0.33805
5b	G(1, 10)	G(2, 2000)	9 (1.00)	5	(*L. v. graecus*, (*L. v. lantzi*, (*L. v. kosswigi*, ((S *L. v. vulgaris*, *L. v. meridionalis*), (*L. v. schmidtleri*, (N *L. v. vulgaris*, (*L. montandoni*, *L. v. ampelensis*)))))); 0.71930
6a	G(2,2000)	G(2,2000)	9 (1.00)	50	(*L. v. meridionalis*, (((*L. v. graecus*, *L. v. lantzi*), (S *L. v. vulgaris*, (*L. montandoni*, *L. v. ampelensis*))), (N *L. v. vulgaris*, (*L. v. schmidtleri*, *L. v. kosswigi*)))); 0.13655
6b	G(2,2000)	G(2,2000)	9 (1.00)	45	((*L. v. graecus*, *L. v. lantzi*), ((*L. v. schmidtleri*, *L. v. kosswigi*), ((S *L. v. vulgaris*, *L. v. meridionalis*), (N *L. v. vulgaris*, (*L. montandoni*, *L. v. ampelensis*))))); 0.12370
7a	G(1, 10)	G(1, 10)	9 (1.00)	3	(*L. v. graecus*, (*L. v. lantzi*, (*L. v. kosswigi*, ((S *L. v. vulgaris*, *L. v. meridionalis*), (*L. v. schmidtleri*, (N *L. v. vulgaris*, (*L. montandoni*, *L. v. ampelensis*)))))); 0.66405
7b	G(1, 10)	G(1, 10)	9 (1.00)	5	(*L. v. graecus*, (*L. v. lantzi*, ((*L. v. schmidtleri*, *L. v. kosswigi*), ((S *L. v. vulgaris*, *L. v. meridionalis*), (N *L. v. vulgaris*, (*L. montandoni*, *L. v. ampelensis*)))))); 0.77125
8a	G(1, 10)	G(2,1000)	9 (1.00)	3	(*L. v. graecus*, (*L. v. lantzi*, ((*L. v. schmidtleri*, *L. v. kosswigi*), ((S *L. v. vulgaris*, *L. v. meridionalis*), (N *L. v. vulgaris*, (*L. montandoni*, *L. v. ampelensis*)))))); 0.80270
8b	G(1, 10)	G(2,1000)	9 (1.00)	9	(*L. v. graecus*, (*L. v. lantzi*, (*L. v. kosswigi*, ((S *L. v. vulgaris*, *L. v. meridionalis*), (*L. v. schmidtleri*, (N *L. v. vulgaris*, (*L. montandoni*, *L. v. ampelensis*)))))); 0.48025

[a] - G(1, 35), G(2, 500): empirically derived priors; G(1, 10), G(2, 2000): large populations with shallow divergence; G(2,2000), G(2,2000): small populations with shallow divergence; G(1, 10), G(1, 10): large populations with deep divergence; G(1, 10), G(2,1000): large populations with intermediate divergence

[b] - starting tree according to consensus phylogeny

[c] - starting tree reflects gene flow among *L. montandoni*, *L. v. ampelensis* and N *L. v. vulgaris*

[d] - starting tree reflects gene flow among N *L. v. vulgaris* and S *L. v. vulgaris*, basal position of *L. v. lantzi*

881

882 **Table 2.** Ensemble genealogical sorting index (*egsi*) for *Lissotriton* operational taxonomic
883 units (10 alleles per group) based on 70 gene trees. All of the P values for *egsi* are <0.000001.
884 The last column provides the number of gene trees in which a group reached complete
885 monophyly.

group	egsi	monophyly
L. v. lantzi	0.692	27
L. v. kosswigi	0.679	30
L. v. graecus	0.564	17
L. v. schmidtlerorum	0.559	14
L. montandoni	0.548	16
L. v. meridionalis	0.497	7
L. v. ampelensis	0.349	0
South *L. v. vulgaris*	0.343	0
North *L. v. vulgaris*	0.281	0

886

887 **Table 3.** Evaluation of fit of mtDNA sequence data to scenarios of incomplete lineage sorting
888 (ILS) and hybridization (Hyb). *Lva – L. v. ampelensis*; *Lvg – L. v. graecus*; *Lvk – L. v.*
889 *kosswigi; Lvm – L. v. meridionalis; Lmon – L. montandoni*; *Lvs – L. v. schmidtleri*; N*Lvv* –
890 North *L. v. vulgaris*; S*Lvv* – South *L. v. vulgaris*

Scenario	Pair of lineages	Minimum divergence - Observed	Minimum divergence – Expected (median of 1000 simulations)	P	Interpretation
mtDNA introgression into *L. montandoni*					
ILS	*Lmon-Lva*	0.0020	0.0010	0.258	O = E
	Lmon -N*Lvv*	0.0000	0.0020	0.294	O = E
	Lmon -Lvk	0.0384	0.0020	0.002	O > E
	Lva-N*Lvv*	0.0020	0.0010	0.220	O = E
	Lva-Lvk	0.0207	0.0020	0.006	O > E
	N*Lvv-Lvk*	0.0374	0.0030	0.002	O > E
	Combined (Fisher's method)			0.00002	data do not fit scenario
Hyb1 *Lmon -Lva*	*Lmon -Lva*	0.0020	0.0010	0.034	
	Lmon -N*Lvv*	0.0000	0.0010	0.500	O = E
	Lmon -Lvk	0.0384	0.0098	0.046	O > E
	Lva-N*Lvv*	0.0020	0.0010	0.242	O = E
	Lva-Lvk	0.0207	0.0098	0.150	O = E
	N*Lvv-Lvk*	0.0374	0.0108	0.066	O = E
	Combined (Fisher's method)			0.0095	data do not fit scenario
Hyb2 *Lmon* -N*Lvv*	*Lmon -Lva*	0.0020	0.0020	0.514	O = E
	Lmon -N*Lvv*	0.0000	0.0000	0.318	O = E
	Lmon -Lvk	0.0384	0.0089	0.040	O > E
	Lva-N*Lvv*	0.0020	0.0020	0.824	O = E
	Lva-Lvk	0.0207	0.0089	0.110	O = E
	N*Lvv-Lvk*	0.0374	0.0098	0.056	O = E
	Combined (Fisher's method)			0.0561	data fit scenario
mtDNA introgression into *L. vulgaris graecus*					
ILS	*Lvg* -S*Lvv*	0.0000	0.0049	0.006	O < E
	Lvg -Lvm	0.0139	0.0059	0.120	O = E
	Lvg -Lvs	0.0208	0.0059	0.036	O > E
	S*Lvv-Lvm*	0.0069	0.0039	0.164	O = E
	S*Lvv-Lvs*	0.0139	0.0049	0.042	O > E
	Lvm-Lvs	0.0396	0.0069	0.022	O > E
	Combined (Fisher's method)			0.0001	data do not fit scenario
Hyb *Lvg*-S*Lvv*	*Lvg*-S*Lvv*	0.0000	0.0020	0.180	O = E
	Lvg-Lvm	0.0139	0.0069	0.086	O = E
	Lvg-Lvs	0.0208	0.0118	0.212	O = E
	S*Lvv-Lvm*	0.0069	0.0069	0.832	O = E
	S*Lvv-Lvs*	0.0139	0.0118	0.560	O = E
	Lvm-Lvs	0.0396	0.0138	0.080	O = E
	Combined (Fisher's method)			0.1152	data fit scenario

891

892

Figure 1. Map with ranges of morphological subspecies (A). Delimitation of evolutionary lineages in the *Lissotriton vulgaris* species group in Structure (B). Pie charts show mean individual cluster membership coefficients. *Lva – L. v. ampelensis*; *Lvg – L. v. graecus*; *Lvk – L. v. kosswigi; Lvl – L. v. lantzi; Lvm – L. v. meridionalis; Lmon – L. montandoni*; *Lvs – L. v. schmidtleri*; N*Lvv* – North *L. v. vulgaris*; S*Lvv* – South *L. v. vulgaris*

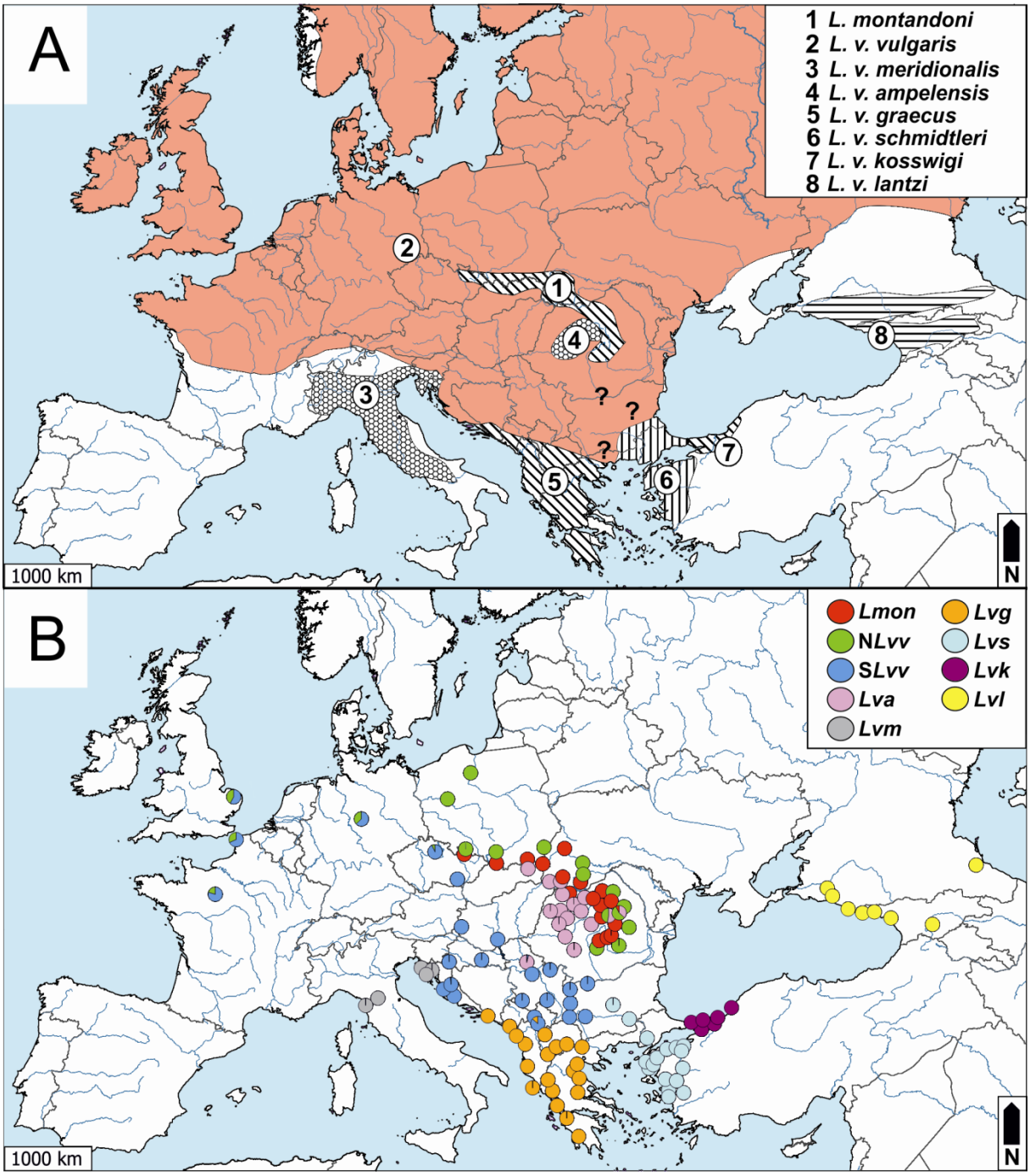

Figure 2. Phylogenetic relationships among STRUCTURE-delimited groups of *Lissotriton* newts; most genetic groups correspond to morphologically defined subspecies (except for *L. v. vulgaris* that is split into northeastern and southwestern lineages and *L. v. ampelensis* which contains two morphologies; see text for details). (A) Majority-rule consensus tree based on 10 replicate analyses (Fig. S4) of 74 concatenated nuclear loci for a total of 36,918 bp; values designate the frequencies of clades found across replicates. (B) Majority-rule consensus of 50 primary concordance trees. Frequency of clades over all replicates (top number) and concordance factors shown as the mean number of loci (out of 70) supporting the clade (± SD). (C) Maximum likelihood tree as inferred by Treemix based on 355 SNPs; horizontal branch lengths are proportional to the amount of genetic drift that has occurred in each lineage. (D) Inferred evolutionary relationships among newt groups by TreeMix with one (left), two (middle) and three (right) migration events. The migration arrows are coloured according to their weights; the weight is correlated with the ancestry fraction.

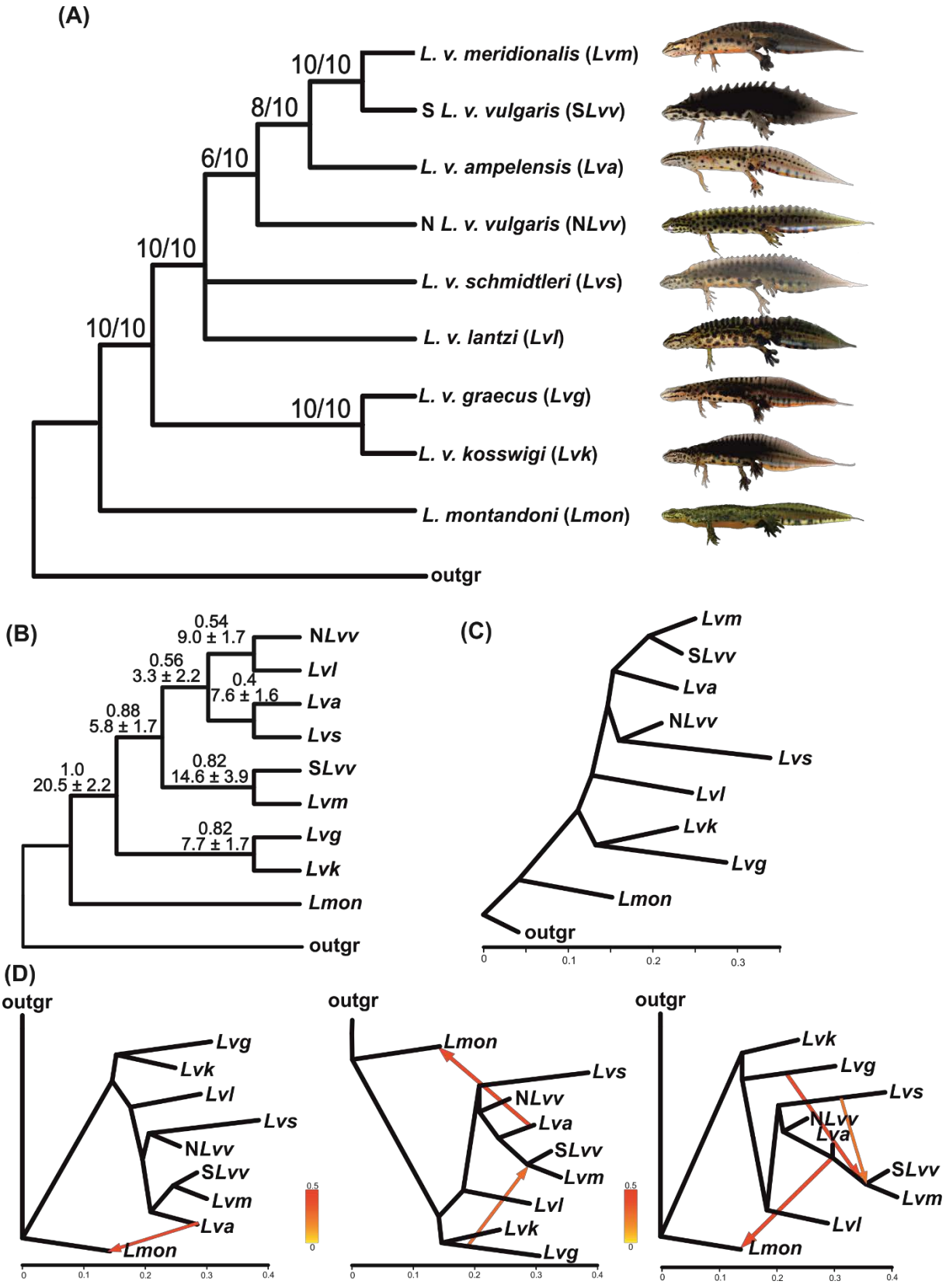

914

915

Figure 3. Top: proportion (in percent, left y-axis and solid circles) of shared haplotypes out of total number of haplotypes summed for each taxon pair across 74 markers; values above solid circles indicate the number of alleles shared by each taxon pair. Bottom: pairwise d_{xy} distances among *Lissotriton* taxa. *Lva – L. v. ampelensis*; *Lvg – L. v. graecus*; *Lvk – L. v. kosswigi; Lvl – L. v. lantzi; Lvm – L. v. meridionalis; Lmon – L. montandoni*; *Lvs – L. v. schmidtleri*; N*Lvv* – North *L. v. vulgaris*; S*Lvv* – South *L. v. vulgaris*

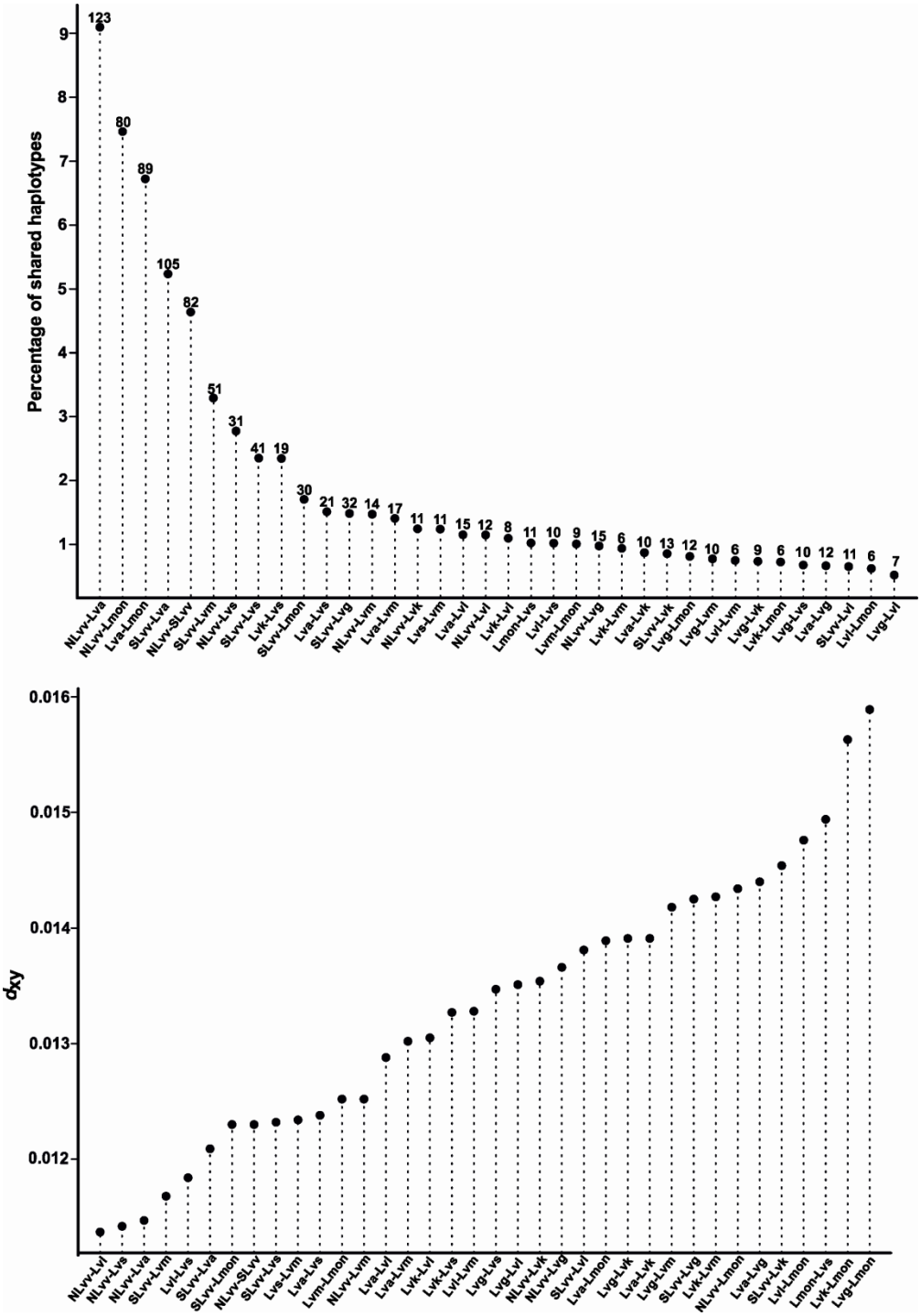

924 **Figure 4.** Pie charts representing posterior distributions of Approximate Bayesian
925 Computation analyses in pairwise taxon comparisons (A), color coded according to
926 demographic models (inset in A). *Lissotriton vulgaris* group phylogeny showing well-
927 supported instances of post-divergence gene flow (green arrows) and their corresponding
928 posterior distributions from the ABC analyses (B).

929

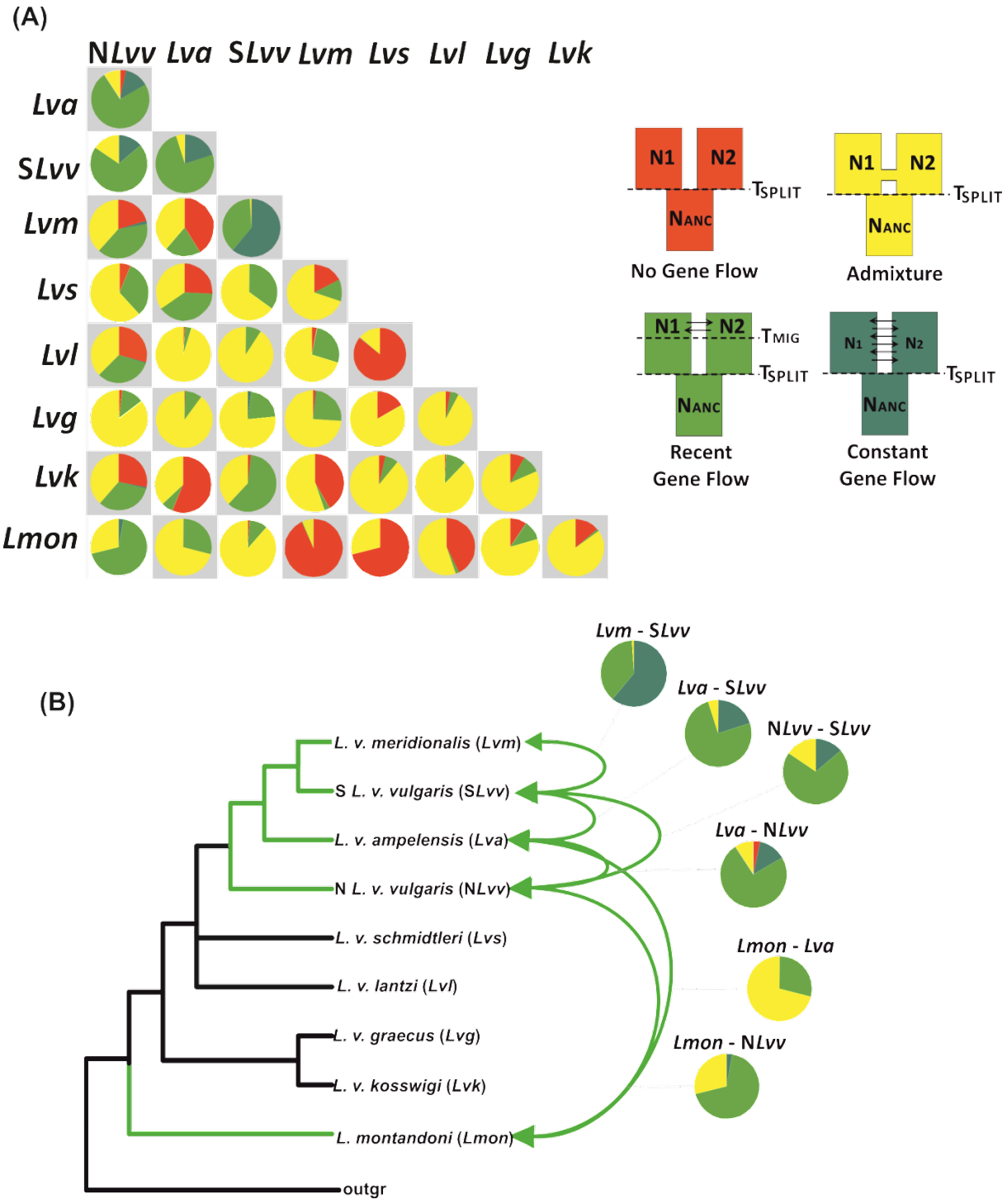

930

931 **Figure 5.** Parameters of species trees under competing scenarios of incomplete lineage
932 sorting (ILS) and hybridization (HYB). Both θ and τ are measured as the expected number of
933 mutations per site.

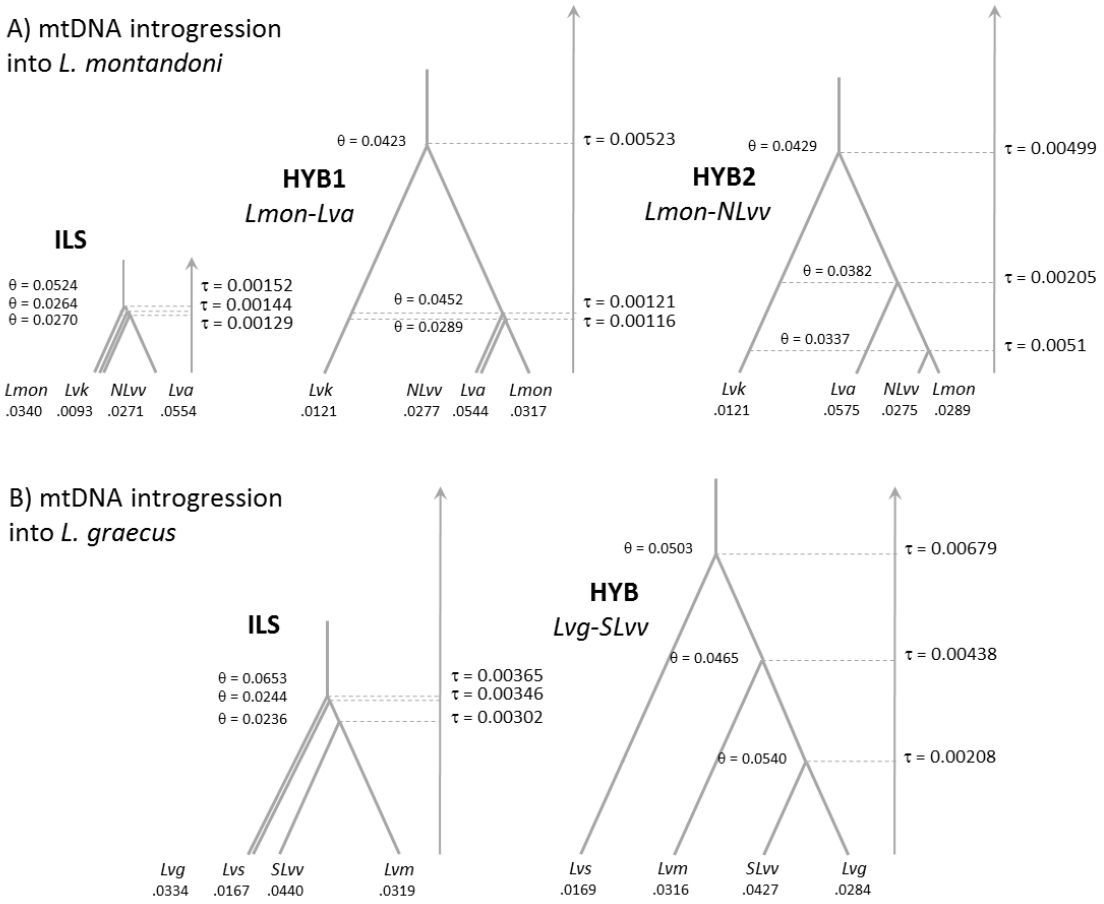

934

935

Supporting Information

Extended Methods: Validation of OTUs in BPP, phylogenetic analysis using BUCKy, *BEAST analyses, and ABC analyses.

Table S1. A list of newt specimens with individual ID numbers, morphological species designation, geographical provenance and estimated proportion of genes in STRUCTURE-defined genetic clusters (c1-c9) representative of the species delimitation proposed in this study.

Table S2. Datasets used for species delimitation and phylogenetic reconstruction.

Table S3. Summary statistics for pairwise comparisons of *Lissotriton* taxa used in Approximate Bayesian Computation analyses.

Table S4. Summary of the nucleotide variation in 74 nuclear markers (mostly 3' UTR regions) in *Lissotriton vulgaris* (including all lineages delimited herein) and *L. montandoni*.

Table S5. Summary of STRUCTURE results for K = 7-12, iterated 10 times each for a total of 60 separate analyses.

Table S6. Pairwise matrix of d_{xy} values calculated for newt OTUs.

Table S7. Results of Approximate Bayesian Computation analyses under four demographic models: no gene flow (NGF), constant gene flow after divergence (CGF), recent (<200 kya) gene flow (RGF), and instantaneous admixture after divergence (ADM).

Table S8. Power analysis for Approximate Bayesian Analyses.

Table S9. Prior and posterior distributions for best model in pairwise taxon comparisons in *Lissotriton* newts from ABC analyses.

Figure S1. Relationships among major mtDNA lineages (denoted by capital letters) in *Lissotriton*, modified from Pabijan *et al.* (2015).

Figure S2. Estimated *Ln* probability of the data for a given *K*, from STRUCTURE HARVESTER; ten replicate analyses were run for each *K*.

Figure S3. Additional substructure found within South *L. v. vulgaris* and *L .v. graecus*.

Figure S4. Consensus trees from 10 replicates of concatenated analyses in MrBayes.

Figure S5. Variation in concordance factors (expressed as the number of genes supporting a particular clade) for main clades found in 50 replicate BUCKy analyses.

Figure S6. *BEAST results including (A) DensiTree diagrams, (B) plots of posterior probabilities for all splits for paired runs of the same analysis revealing consistency in retrieving the same species tree topology, and (C) 95% highest posterior density intervals for three key parameters (log likelihood, posterior and species tree height) from *BEAST analyses compared for paired runs.

Figure S7. Scaled residual fit from the TreeMix analysis based on the maximum likelihood tree in Fig. 2C (no migration edges).